INTEGRATED 3D ACID FRACTURING MODEL FOR CARBONATE RESERVOIR STIMULATION

A Thesis

by

XI WU

Submitted to the Office of Graduate and Professional Studies of
Texas A&M University
in partial fulfillment of the requirements for the degree of

MASTER OF SCIENCE

Chair of Committee,	Eduardo Gildin
Co-Chair of Committee,	Ding Zhu
Committee Members,	Alfred Daniel Hill
	Yuefeng Sun
Head of Department,	Alfred Daniel Hill

August 2014

Major Subject: Petroleum Engineering

ABSTRACT

Acid fracturing is one of the stimulation methods used in carbonate formations and has been proved effective and economical. Because of the stochastic nature of acidizing in carbonate formation, designing and optimizing acid fracture treatment today still remain challenging. In the past, a simple acid fracture conductivity correlation was usually considered sufficient to estimate the overall average fracture conductivity in the formation, leading to the computation of the productivity index for fractured well performance. However, the nature of heterogeneity could not be included in the modeling. Understanding the important role of heterogeneity to stimulation performance becomes a crucial step in design and optimization of acid fracture jobs. In order to study the effect of this stochastic nature on acid fracturing, a fully 3D acid reaction model was developed based on the geostatistical parameters of the formation. It is possible to describe local conductivity distribution related to acid transport and reaction process. In this study, we have developed a new interactive workflow allowing the model of the fracture propagation process, the acid etching process and the well production interactively. This thesis presents the novel approach in integrating fracture

propagation, acid transport and dissolution, and well performance models in a seamless fashion for acid fracturing design.

In this new approach, the fracture geometry data of a hydraulic fracture is first obtained from commercial models of hydraulic fracture propagation, and then the 3D acid fracture model simulates acid etching and transport from the fracture propagation model using the width distribution as the initial condition. We then calculate the fracture conductivity distribution along the created fracture considering the geostatistical parameters such as permeability correlation length and standard deviation in permeability of the formation. The final step of the approach is to predict well performance after stimulation with a reservoir flow simulator. The significant improvements of the new approach are two folds: (1) capturing the geostatistical effect of the formation; and (2) modeling the acid etching and transport more accurately. The thesis explains the methodology and illustrates the application of the approach with examples. The results from this study show that the new model can successfully design and optimize acid fracturing treatments.

DEDICATION

I dedicate this thesis to my beloved mother and father, who are always my biggest fans and supporters. I also dedicate this thesis to my adorable cat, kissy baby, for her long-time companionship.

ACKNOWLEDGEMENTS

I would like to thank my advisers, Dr. Zhu, Dr. Gildin and Dr. Hill, for their patience, encouragement, and technical support of this work. They adopted me into this industry and have provided everything I needed.

Cassandra Oeth's work is to be commended for providing the basis of this research project. Her generous help and insightful advises are appreciated. And I would like grant my general thanks to all my colleagues in the research group and department for assistance on this project.

Thanks also go to my dear roommate Jiaqi Zhang and best friend Anqi Guo. Without their encouragement and therapy, I won't get rid of those downcast time as quickly as I did.

I also want to extend my gratitude to the Acid Fracture Joint Industry Project and Crisman Institute for consistent financial support of this work.

Lastly and most importantly, thank you to my parents. Because of you, I am who I am.

NOMENCLATURE

E	Young's modulus, Mpsi
$f_{calcite}$	Percentage of calcite
k_f	Fracture permeability, md
w	Fracture width, in
$\bar{w}$	Average etched fracture width, in
w_i	Ideal etched fracture width, in
wk_f	Fracture conductivity, md-in
$(wk_f)_0$	Fracture conductivity at zero closure stress, md-in
α, β	Correlation constants for fracture conductivity
λ_{Dx}	Normalized correlation length along fracture length
λ_{Dz}	Normalized correlation length along fracture height
σ_c	Closure stress, psi
σ_D	Normalized standard deviation

TABLE OF CONTENTS

LIST OF FIGURES

LIST OF TABLES

CHAPTER I

INTRODUCTION

1.1 Background

Carbonate formations are usually highly fissured. For low permeability carbonate formations, stimulation is needed to enhance well productivity. Acid fracturing is a well stimulation technique for carbonate formations. In an acid fracturing treatment, a hydraulic fracture is first created in the formation by pumping fracture fluid at a pressure higher than the fracture breakdown pressure. Then acid is injected to the created fracture. The acid dissolves rock along the faces of hydraulically induced fractures and creates conductivity after fracture closure (Ruffet *et al.*, 1998; Pournik *et al.*, 2007; Economides *et al.*, 2012). Figure 1.1 shows the whole procedure of an acid fracturing in carbonate formation. Because of naturally occurring heterogeneities, some parts of the fracture surface will react more with the acid than others, resulting in a deeper etching of the fracture wall at these points. Such uneven etching is the mechanism of conductivity in acid fracturing. Figure 1.2 shows a heterogeneous permeability distribution on the surface before acid-fracturing treatment. It shows characteristics of strong-spatial correlation in acid flow direction

in general. Correlated permeability in flow direction results in higher conductivity than randomly distributed permeability. (Mou *et al.*, 2009)

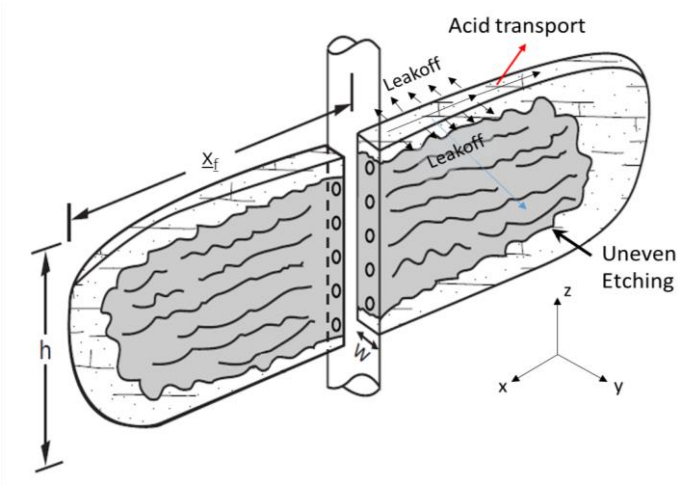

Figure 1.1 Acid fracture in carbonate

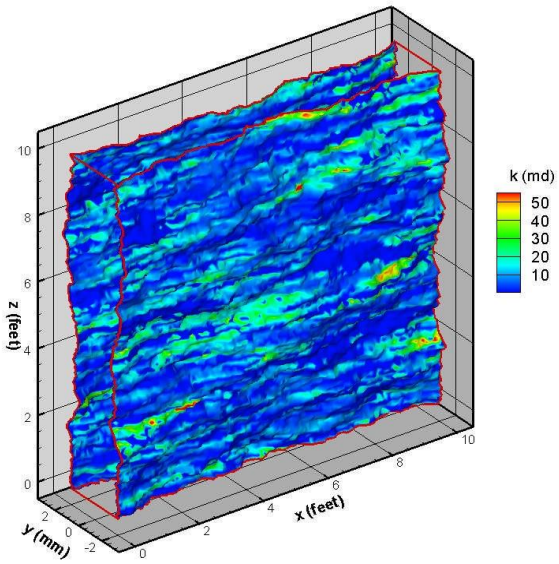

Figure 1.2 Heterogeneous permeability distribution
(Reprinted with permission from Paper SPE 119619: "Acid-Etched Channels in Heterogeneous Carbonates—A Newly Discovered Mechanism for Creating Acid Fracture Conductivity" by Mou, J., Zhu, D. and Hill, A.D. 2009. Copyright 2009 by SPE)

An etching pattern occurring on the fracture surface is a dominant factor for fracture conductivity. A systematic experimental study illustrated that, once the channel created by acid etching in preferred pathway resulted from heterogeneities, it tends to remain open and retain conductivity after closure. (Melendez *et al.*, 2007)

Current acid fracture models predict fracture conductivity based on the assumption of uniform dissolution pattern, and created conductivity is calculated using the extrapolation of small scale laboratory measurements (Mou *et al.*, 2009). To solve this issue, Deng *et al.* (2012) established a set of new correlations incorporating the effect of spatial distributions of formation properties to calculate conductivity after acid etching process and fracture closure. Accordingly, a fully 3D simulator using Deng's conductivity correlations was developed to simulate acid transport and reaction and predict the performance of acid fracture. The new acid fracturing simulator is able to grid the domain in the fracture width direction, which allows to capture the changes in acid concentration (Oeth *et al.*, 2013). With all these advances, an integrated model for acid fracturing considering fracture propagation and acid transport and reaction becomes necessary.

1.2 Literature Review

1.2.1 Acid Fracturing Model

An acid fracturing process consists of fracture propagation and acid transport and acid-reaction. This process can be described by a fracture propagation model and an acid transport/ reaction model which are intrinsically coupled. Many models and approaches are developed in the past. Because of the complexity, acid transport/reaction model is usually not coupled with a fracture propagation model. Acid transport/reaction model is commonly replaced by a correlation to estimate conductivity of a fracture.

Lo and Dean (1989) built the first numerical model of acid fracturing stimulation. They applied incompressible laminar steady-state flow, constant leakoff rate, and no gravity effect as model assumptions. A one-dimensional approximation method with averaged acid concentration over the fracture width direction was used in the model to solve the two-dimensional convection diffusion equation.

Antonin Settari (1993) developed a comprehensive acid-fracturing model. He assumed that acid viscosity is not a function of acid concentration, and acid flow in the fracture height direction is neglected. His model achieved in using mass transfer and rate of reaction rate to control the acidizing process, simulating multiple fluids

with different rheologies, and accounting for the influence of mass transfer coefficients caused by the increment of leakoff.

Ruffet *et al.* (1998) characterized the etched surfaces quantitatively and evaluated their relation with acid injection conditions. In their approach, Ruffet *et al.* measured the 2D surface profile with a mechanical profile meter after each etching experiment and used these digital data to calculate the statistical measurements of the data distribution and the linear and absolute roughness values. Their global roughness parameter encapsulated all these measurements to compare among different treatment conditions. In addition, Ruffet *et al.* estimated the mechanical behavior of the surface under closure stress, using digitalized profile data to calculate specific topographic descriptors, which are used to estimate the fracture conductivity behavior.

The acid concentration in the fracture width direction is necessary to calculate the acid transport to the fracture wall. Unfortunately, lacking the calculation of concentration gradient over the fracture width direction, the models mentioned above simplified acid transported to fracture walls by using mass transfer coefficient.

To improve the acid fracture model, Settari *et al.* (1998) presented a two-dimensional acid transport model which solves the flow in fracture length and width directions and neglects variation in fracture height direction. He made assumptions

that the reaction has no effect on volumetric flow rate, acid concentration in vertical direction is uniform and fully developed flow profiles at every point in the fracture. In their model, the velocities could be calculated from the average flow rate computed by the flow/geometry model and fluid properties.

Simulating acidizing in a natural fractured carbonate reservoirs, Dong (2001) developed an unsteady-state two-dimensional model considering rough fracture surfaces and two-dimensional fluid flow (the fracture length and height directions). Acid transported to the fracture walls was also calculated by using a mass transfer coefficient.

Acid/rock reaction is a heterogeneous process while acid is being transported to the rock surface. Mou *et al.* (2009) developed a two dimensional intermediate-scale acid fracture model. In their model, "small grid sizes are utilized to capture the local heterogeneity while the total dimension is large enough to capture the macro-scale heterogeneity". The model also calculates velocity fields, acid concentration distributions, and fracture surface profiles by solving Navier-Stokes equations, acid balance equations, and acid/rock reaction. They studied how the heterogeneous permeability and mineralogy affect the facture surface etching patterns, which determines conductivities.

Deng *et al.* (2012) built a set of correlations to predict the acid fracture conductivity based on Mou's work. The new correlations in three categories could calculate the conductivity on an intermediate scale, closing the gap between the macroscale simulators and the microscale experiments. The acid transportation and the deformation on the surface of fracture are modeled under closure stress. The detailed correlation will be discussed in the model description section. Figure 1.3 describes the work flow of Deng's models.

Oeth *et al.* (2013) developed a novel three-dimensional acid transport and etched model, considering the heterogeneity and fluid dynamics. There are several features that differ from the previous models. It grids the fracture in all three dimensions which allows to capture the changes of acid concentration maps occurring across the fracture. The example of the acid profile is shown in Figure 1.4. Etching calculated from the concentration profiles yields the conductivity of the fracture by the new conductivity correlations (Deng, 2012). Computational fluid dynamics was firstly used in this model to describe the three-dimensional profile of acid throughout a fracture to quantify the etching.

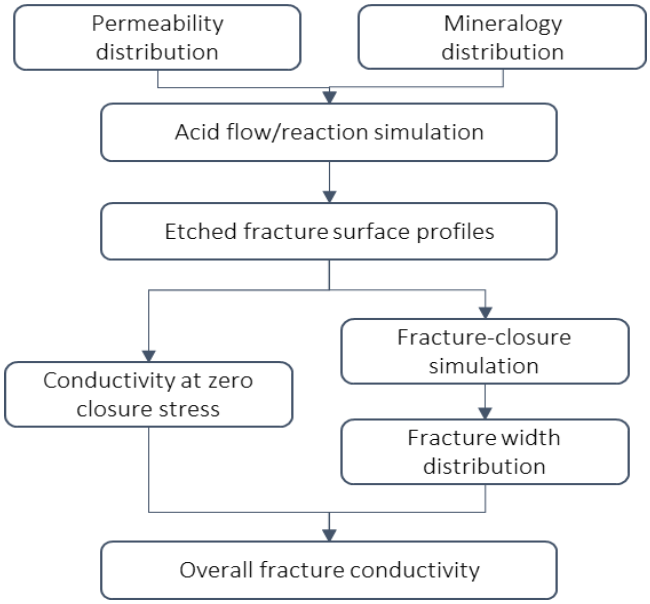

Figure 1.3 Computational procedure of Deng's models

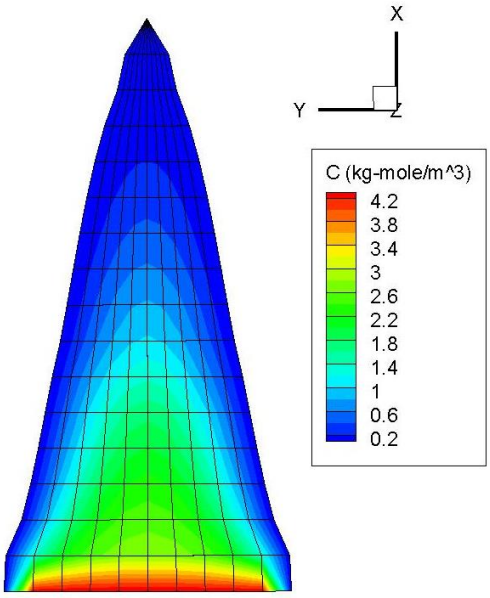

Figure 1.4 Acid concentration map of Oeth's simulator (Reprinted with permission from Paper SPE 168602: "Acid Fracture Treatment Design with Three-Dimensional Simulation" by Oeth. C. V., Hill, A.D. and Zhu, D., 2013. Copyright 2013 by SPE)

1.2.2 Coupling Method

Researchers recognized the importance of multiple models to fracture performance. Model coupling was first proposed in the early 1980s (Settari, 1980; Hagoort *et al.*, 1980; Nghiem *et al.*, 1984).

Hagoort *et al.* (1980) developed a mathematical reservoir model to simulate the propagation of waterflood-induced hydraulic fractures in a symmetry element of a waterflood pattern. The model consists of a conventional single-phase reservoir simulator coupled with an analytical fracture model. The model is capable of simulating fracture propagation as a function of injection and production rates or pressures, reservoir and fluid properties, and formation-fracturing pressures.

Antonin Settari (1980) then developed a numerical model of the fracturing process with considering the fracture mechanics, flow, and heat transfer. Fracture mechanical and propagation models are coupled. The discussion is limited to vertical fractures for its prevalence.

This methodology has been further developed by Ji and Settari (2007) to combine a reservoir model, a geomechanical model, and a fracture geometry model by using the same grid system to model each part. Their model can handle simultaneously a 3-D planar fracture growth, poroelastic effects, varying fracture conductivity and fracture volume in the reservoir model. Fracture volume is

recognized as an important factor in the fracture propagation process. They also considered that poroelastic effect plays as a crucial factor, especially for leakoff-dominated situation (low fluid efficiency) where strong stress changes result from high pore pressure changes caused by high leakoff.

Samier *et al.* (2007) presented a technique for introducing geomechanical effects within a conventional reservoir simulator. They developed a new coupling scheme that could couple a standard geomechanical analysis tool and a standard reservoir simulator without any specific modification. At user-defined steps, the fluid pressures are transmitted to the geomechanical tool, which computes the actual stresses and reports the modifications of porosities and permeabilities back to the reservoir simulator.

1.3 Objectives

The objective of this project is to develop a tool to design and analyze acid-fracturing treatments by integrating multiple models in one simulation platform. This includes a fracture propagation model (geomechanics model), an acid transport and reaction model, a fracture conductivity model, and a reservoir performance simulation model. This work aims at developing an integrated approach of acid fracture modeling that closes the gap between laboratory-scale measurements of acid

fracture conductivity and macro-scale acid fracture models to the performance of an acid fractured well.

To this end, the main tasks developed here are:

1. Generate fracture geometry by an existing fracture geomechanics model.
2. Couple the fracture model with the acid model linking the acid model with the geometry generated by the fracture model to create fracture conductivity.
3. Estimate well performance from the conductivity generated by the acid model.
4. Verify the accuracy of the result by employing this approach in both simplified sample and field case.

CHAPTER II

MODEL DESCRIPTION

2.1 Introduction

Acid fracturing stimulation involved several interactive procedures: fracture opening, fracture growth, acid injection, acid transport in the fracture, acid dissolution on the fracture surface, fracture closure and well production. Reorganizing by the functions of models, we considered fracture geometry model, acid transportation and dissolution model and well performance model as components of a three-step integrated simulation framework.

2.2 Fracture Propagation Model

Geomechanics models simulate fracture propagation in an in-situ stress field when high-pressure injection is introduced to the rock. Under a given injection condition, the geomechanical model calculates fracture geometry in three dimensions as a function of injection. Geomechanical models can be simplified to two-dimensional models when assuming a constant height exists during injection; they can also be viewed as Pseudo three dimensional models when height growth is a step

function based on vertical stress contrast; and finally as fully three dimensional models. Fracture propagation models have been accepted by the industry. Many of them became standard design tools. We adopted four different fracture models in this work to calculate fracture dimensions before acid injection. Two of them, Fracpro (Fracpro, 2011) and MFrac (Meyer, 2012), are pseudo 3D models, and the other two, E-StimPlan (NSI Technologies Inc., 2010) and GOHFER (GOHFER, 2012), are planner 3D models. These models are run for non-reactive fluid before acid injection, and the fracture width is then used as the initial condition in acid transport and dissolution modeling.

In what follows, we make a brief description of these commercial software used in this work.

2.2.1 Fracpro

Fracpro is a Pseudo-three-dimensional hydraulic fracturing model. This model was first presented by Settari and Cleary (1986). It is less comprehensive but more practical. The geometry model is based on a 3-D Lumped Fracture Model (Settari *et al.*, 1986), however have some modification by introducing shape factors, i.e. fracture toughness, stress profile, modulus, leak-off, etc., as multiplier into the model. The Pseudo-3D model is formulated using the equations underlying for fluid flow and crack opening for the

main body of the fracture and are coupled with a scheme for describing the vertical fracture growth at each cross section (y-z plane, where *y* stands for width opening direction and *z* stands for height direction). Figure 2.1 shows the fracture profile generated by Fracpro. The left part is the half wing profile (x-z plane, where x stands for fracture length direction) of proppant concentration in the fracture. The width opening is shown on the right side. The reaction to the stress change from layer variation is demonstrated by the width distribution, as it shown in Figure 2.2.

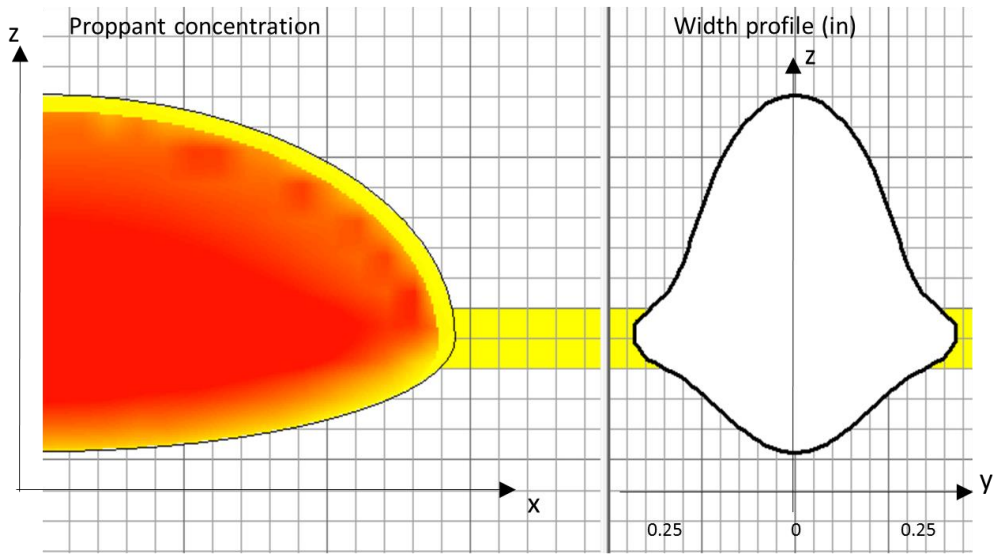

Figure 2.1 Fracture profile and proppant concentration in Fracpro

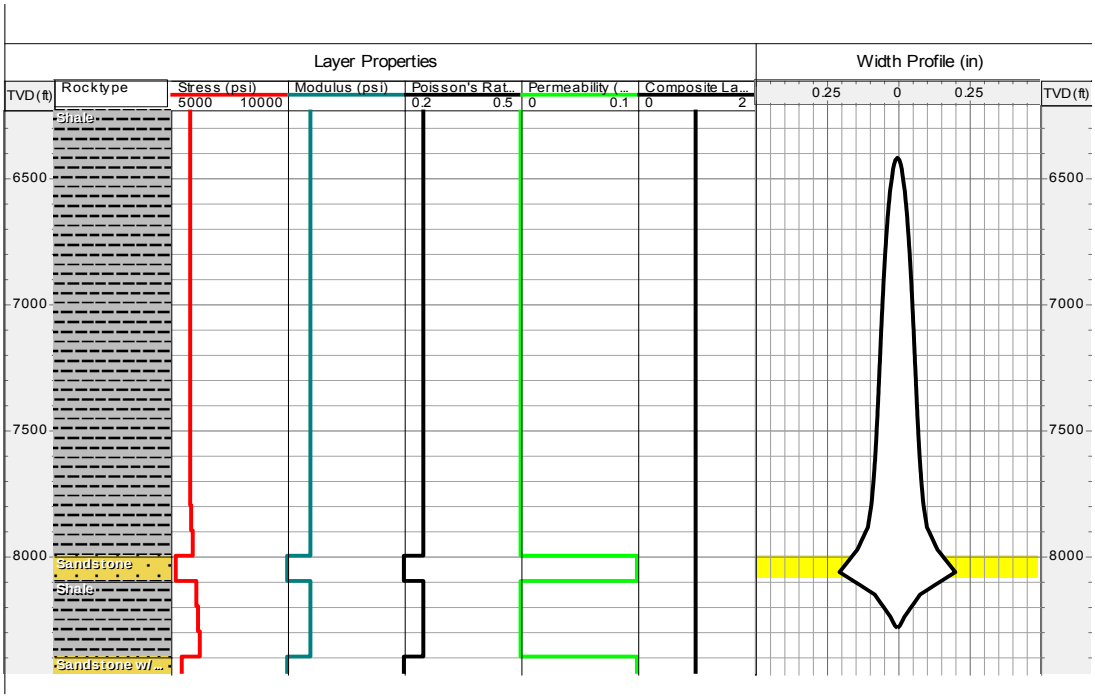

Figure 2.2 Fracture width versus stress profile in Fracpro

2.2.2 MFrac

A three-dimensional planar fracture model with either lateral or vertical fracture propagation is modeled in MFrac. Simulating large length to height aspect ratio cases, the model approaches the PKN model which has constant height type geometry. When no confining stress, toughness or moduli contrast are encountered, the model approaches vertical radial-shape fracture geometry. MFrac also accounts for the coupled parameters affecting fracture propagation and proppant transport.

MFrac is not a fully 3-D model. It is however, formulated between a pseudo-3D and a full 3-D type model with an applicable half-length to half-height aspect ratio greater than about 1/3. It also has options for 2-D type fracture models. Figure 2.3 shows the typical fracture geometry output in MFrac. Crack opening reflects the stress variation.

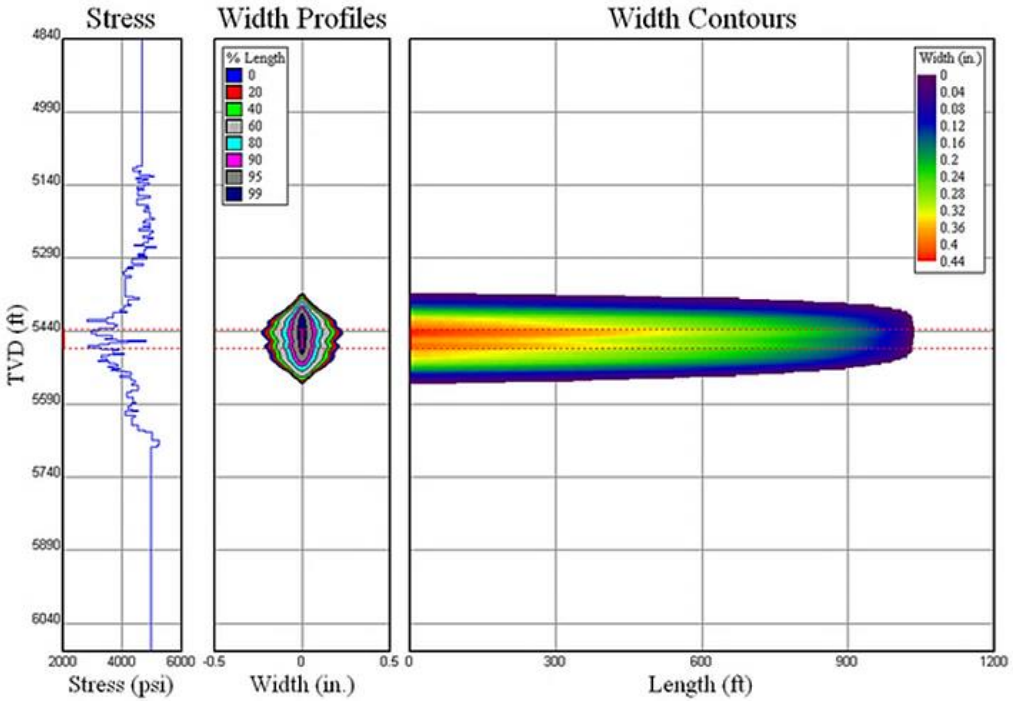

Figure 2.3 Typical fracture geometry output in MFrac

2.2.3 GOHFER

GOHFER, which stands for Grid Oriented Hydraulic Fracture Extension Replicator, is a planar three dimensional geometry fracture simulator with a fully coupled fluid/solid transport simulator. The model utilized Cartesian corner point gridding system to describe the entire domain, similar to a reservoir simulator approach. Fluid composition, proppant concentration, shear, leakoff, width, pressure, viscosity and other state variables are defined at each corner point of grid blocks. The fracture extension and deformation model in GOHFER is based on a formulation that expects the formation to fail in shear.

In GOHFER, the in-situ stress is internally calculated from pore pressure, poroelasticity, elastic moduli and geologically consistent boundary conditions. Local displacements are controlled by local pressures and rock properties. An output example is presented in Figure 2.4.

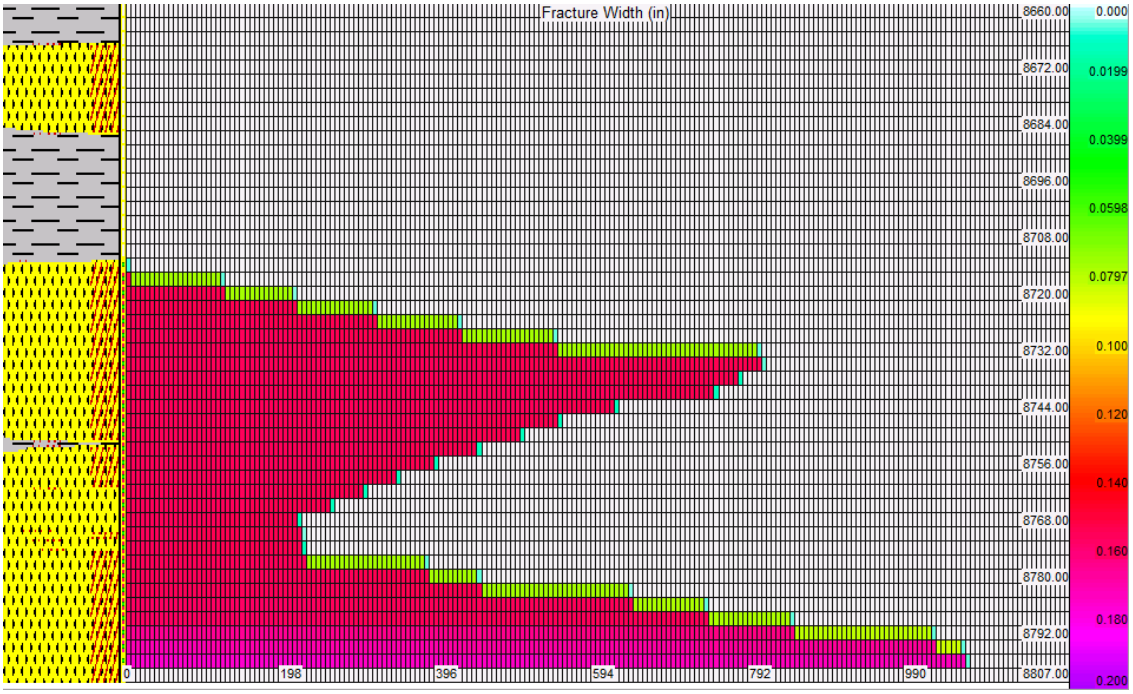

Figure 2.4 The example fracture width profile in GOHFER

2.2.4 E-StimPlan

E-StimPlan is a 3-D fracture geometry simulator, though the fracture is still constrained to lie in a single plane. It includes a rigorous, fully numerical solution for two dimensional fluid-flow/proppant-transport calculations and a rigorous FEM (Finite Element Method) solution for fracture width and propagation in a layered formation with varying moduli. It also has 1-D and 2-D options in E-StimPlan. The fracture geometry simulated by E-StimPlan is presented in Figure 2.5.

E-StimPlan differs from the Pseudo-3D models due to the following two enhancements. Fracture width is calculated by using 3-D elasticity, and, is a function of pressure everywhere in the fracture zone. Thus, the fracture width is calculated correctly for a complex geometry. Secondly, fracture propagation is allowed and calculated for any points around the fracture perimeter. Thus, when the fracture breaks through into another layer with lower stress the fracture begins to preferentially propagate into that zone.

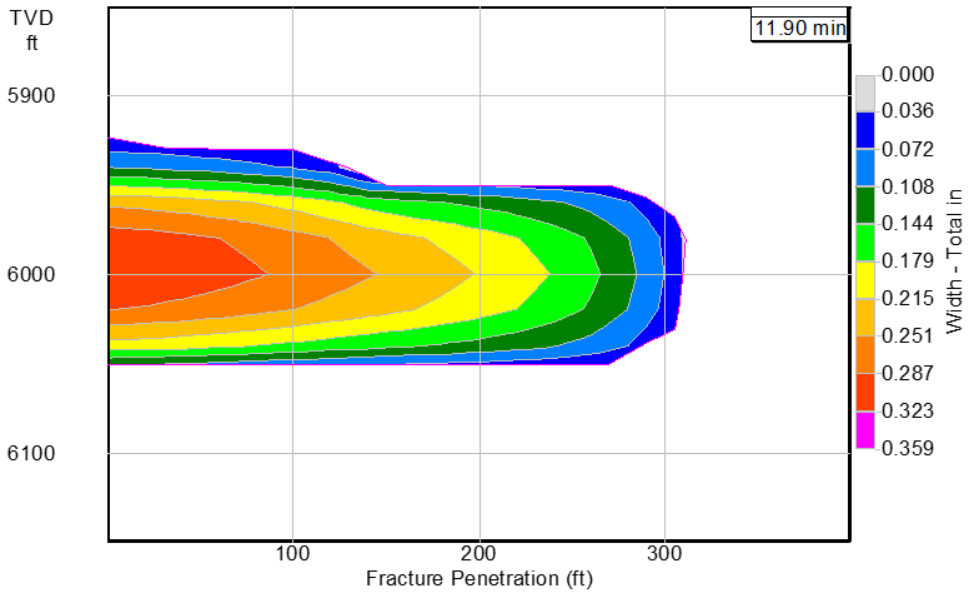

Figure 2.5 Fracture contour map generated by E-StimPlan

From the models mentioned above, the fracture initial geometry data is calculated and provided to the acid fracture model as initial condition to solve acid

transportation and reaction. The coupling of each individual model will be discussed in the next chapter.

2.3 Acid Transport and Dissolution Model

Differential etching from the uneven dissolution of the fracture faces is expected to create the conductivity after closure. The uneven etching can be initiated from permeability distribution, mineralogy distribution and initial width, or the combined effects of all three. A fully three-dimensional model is capable of incorporating the formation rock properties (permeability and/or mineralogy) distribution along the fracture faces, and also to solve acid diffusion and convection in the fracture width direction (Mou *et al.*, 2010; Oeth, *et al.*, 2013). This approach allows the dynamic acid concentration to be resolved in three dimensions throughout the fracture. The acid concentration profile by chemical diffusion or physical convection determines the acid distribution at the fracture surface. The acid front reaches the fracture wall and reacts with the formation rock, creating an uneven surface due to the statistical distribution of the formation rock properties.

The acid fracture simulator yields the amount of dissolution that has occurred in every fracture grid block. With this information and a description of the statistical

variations of the rock properties, a correlation developed by Deng *et al.* (2012) for acid fracture conductivity, wk_f, can be computed by,

$$wk_f = \alpha \exp\left[-\beta\sigma_c\right] \tag{1}$$

where α and β are defined based on the formation geostatistical characteristics. If permeability distribution dominates acid etching and resulting conductivity, then

$$\alpha = 0.12\left(wk_f\right)_0\left(\lambda_{D,x}\sigma_D\right)^{0.1}, \tag{2}$$

and

$$\beta = \left[15.6 - 4.5\ln\left(\sigma_D\right) - 7.8\ln\left(E\right)\right]\times 10^{-4}. \tag{3}$$

If mineralogy distribution dominates the process, then

$$\alpha = \left(wk_f\right)_0\left(0.811 - 0.853\, f_{\text{calcite}}\right), \tag{4}$$

and

$$\beta = \left[1.2\exp\left(0.952\, f_{\text{calcite}}\right) + 10.5E^{-1.823}\right]\times 10^{-4}. \tag{5}$$

Finally if permeability and mineralogy distributions have similar impact on the conductivity, then

$$\alpha = \left(wk_f\right)_0\left[0.21\lambda_{D,x}{}^{0.16} + 0.046\ln\left(\sigma_D\right) + 0.15\lambda_{D,z}{}^{-0.17}\right], \tag{6}$$

and

$$\beta = \left[53.8 - 4.58\ln\left(E\right) + 18.9\ln\left(\sigma_D\right)\right]\times 10^{-4}. \tag{7}$$

For the permeability dominated case, the conductivity at zero stress,$(wk_f)_0$, is calculated by

$$\left(wk_f\right)_0 = 4.48\times 10^9\,\overline{w}^3\left[1 + \left(a_1 erf\left(a_2(\lambda_{D,x} - a_3)\right) - a_4 erf\left(a_5(\lambda_{D,z} - a_6)\right)\right)\sqrt{(e^{\sigma_D} - 1)}\right], \tag{8}$$

$$a_1 = 1.82 \qquad a_2 = 3.25 \qquad a_3 = 0.12 \qquad a_4 = 1.31 \qquad a_5 = 6.71 \qquad a_6 = 0.03.$$

and for uniform mineralogy

$$\overline{w} = 0.2 erf\left(0.78\sigma_D\right) w_i^{0.81}. \tag{9}$$

In the above equations, permeability correlation length λ_{Dx} and standard deviation of permeability σ_D are geostatistical properties of the formation; and Young's modulus E, closure stress σ_C and calcite content $f_{calcite}$, are rock mechanics properties of the formation. w is the fracture width and w_i is the ideal acid-etched width. The fracture width at zero closure stress is provided by the fracture models discussed.

2.4 Well Performance Model

To predict the effectiveness of an acid-fracture treatment, we need a reservoir flow model that connects the conductivity of an acid-fractured well to the productivity. To retain the detailed description of an acid fracture, we use a multi-phase, 3-D reservoir simulation to complete the approach. In this work, a black-oil simulation model is built using ECLIPSE (Schlumberger, 2011). In this work, we use only an oil-water model, however, the gas options are also available. ECLIPSE provides free format input method with a keyword system, allowing users to describe a formation with existing designed fractures. Thus, we are able to transfer the conductivity distribution from acid etching model by decoupling it into fracture width and permeability. With the same grid system as the acid fracturing model, the reservoir simulation inherits the formation parameters (permeability, porosity,

young's modulus, critical crack opening pressure, etc.). Figure 2.6 shows the example of the production declined curve predicted by the reservoir model. We could also observe the cumulative production, the formation pressure changes, the oil saturation distribution, etc. in ECLIPSE. From this predicted production history, the treatment design can be evaluated and optimized.

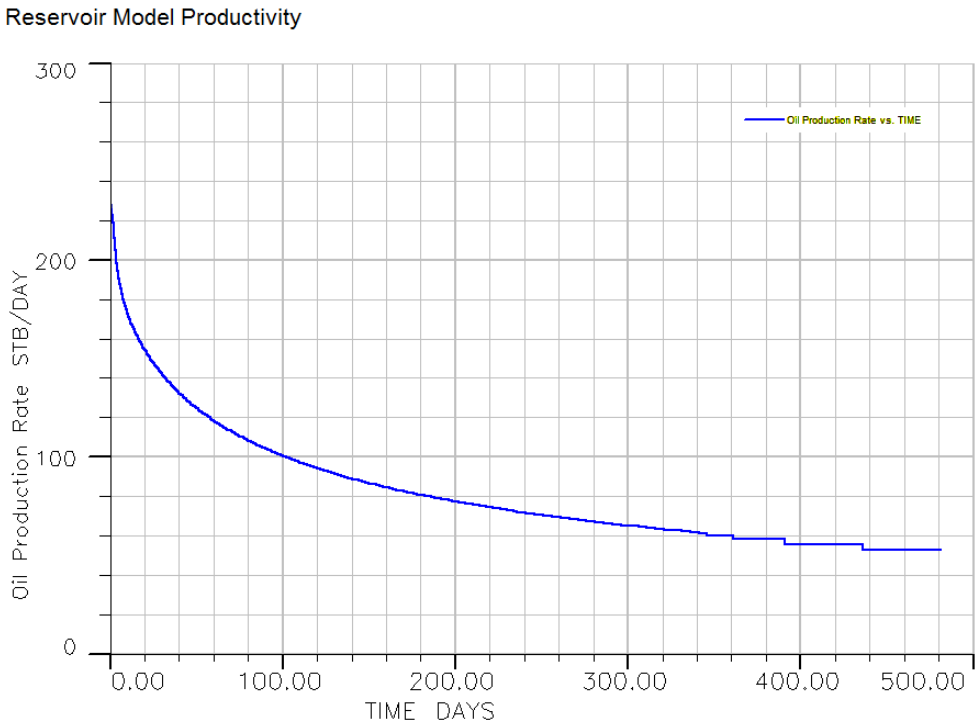

Figure 2.6 Production rate calculated by Eclipse

CHAPTER III

METHODOLOGY

This chapter describes the coupling approach. The models introduced in Chapter II will be integrated in a seamless fashion. The connection and transformation will be discussed in detail.

3.1 Coupling Method

The idea of transferring the shared data to associate two distinctive models, named coupling method, was first proposed in early 1980s (Settari 1980; Hagoort *et al.* 1980; Nghiem *et al.* 1984). Generally, we can divide the coupling techniques into two main branches: one-way coupling and interactive coupling. In the interactive coupling scheme, for example, the coupling between the fracture propagation model and the acid transport and reaction model, the fracture geometry variables (fracture height, half length, width) and acid transport and reaction variables (etched width) are calculated separately and sequentially, by a fracture propagation model and an acid fracturing model, respectively. These parameters are exchanged at each time step until convergence is reached. The one-way coupling on the other hand, is based on the computation of each model independently and thus, we only transfer the shared

parameters once from one model to another into the framework. The results from the consequential model will not be sent back to the previous model. The main scheme of these approaches is to employ only the important shared variables into models, such as pressure, permeability, deformation volume, etc.. This work use height h, fracture half-length x_f, and width w(x,z) as coupling parameters. Ideally, interactive coupling runs the acid model with the boundary condition inherited from the fracture model to calculate etched width distribution, and then embeds the width distribution back to the fracture model. The two models are coupled to solve both fracture growth and acid transport together during the acid injection. After the treatments, we use the conductivity to transfer the acid fracture to a reservoir simulation model to predict its final productivity.

To accomplish interactive coupling, we need to be able to go back and forth with parameters exchange, and therefore access to each model involved into the process. In this work, the fracture geometry is generated by commercial software packages. Sending data back to the fracture models and requiring a "restart" with the geometry data provided by users may not be available. Currently, this work uses one way coupling assuming that the fracture will not further grow during acid and the acid etched effect will not affect the response calculated by the fracture geometry model. In summary, geometry information, such as height h, fracture half-length x_f,

and width $w(x,z)$, are sent to the acid transport and reaction model, then the results resolved by the acid model are transferred to the reservoir simulation model to predict the production performance. Figure 3.1 summaries the paradigm of the coupling method we designed for this work.

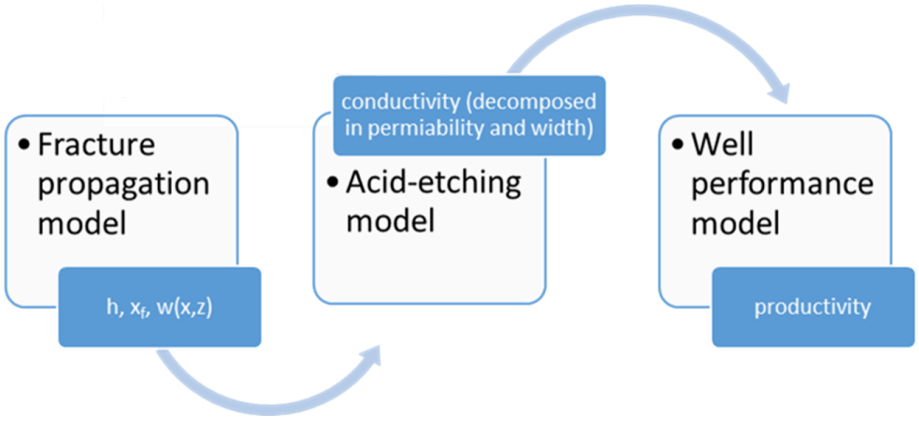

Figure 3.1 Scheme of coupling method in this work

3.2 Gridding System

The three models that are going to be coupled (the fracture geometry model, the acid model and the reservoir model) have different gridding-structures, and the first step of the coupling algorithm is to obtain a consistent grid system.

In the 3D fracture model, it is common that a regular Cartesian eight-node corner point geometry (CPG) gridding system is used, while Cartesian center point brick-shaped elements are used in the acid transport and reaction simulation and the

reservoir flow simulation within the finite difference method. Figure 3.2 shows the Cartesian eight-node corner point gridding system and the Cartesian center point gridding system. The transfer is needed between two different gridding systems. If the width is generated from a fracture geometry model using the Cartesian eight-node corner point gridding system, then the corner properties at eight nodes are averaged over the grid and the average value is assigned to the center point of the grid. In this work, the fracture geometry is output at the corners of the cells, and the acid model requires the average width located between these nodes to populate each grid block. The average of the neighboring nodes of the fracture propagation model output width across the fracture height and length is what is input to the acid model.

This methodology ensures the consistent transition between models. The grid is set in the fracture model; the acid transport and dissolution model and the reservoir simulation model use the same gridding system as the fracture model.

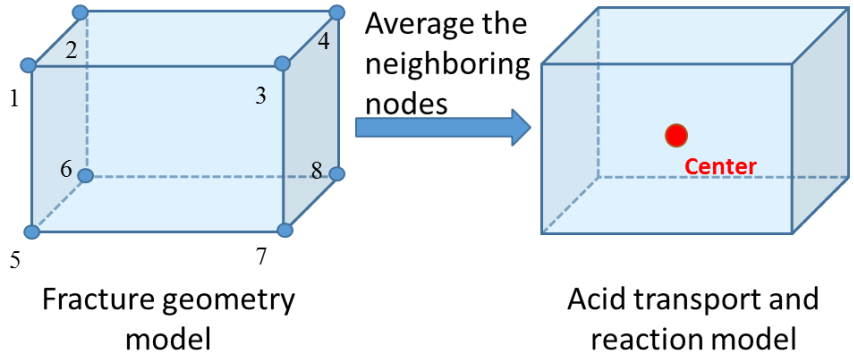

Figure 3.2 Cartesian eight-node corner point gridding compare with center point gridding

3.3 Work Flow

The integration workflow is illustrated in Figure 3.3. The approach starts with a fracture simulator, which uses a geomechanical model, to calculate fracture width during the pad injection. A hydraulic fracture is created at the defined injection condition. Next, we transfer the fracture geometry along to the acid fracture model. Other input data needed are such as flow rate, acid concentration, and power-law parameters. The acid fracture model simulates acid transportation and etching on the fracture wall to create an uneven surface at the fracture walls under the defined condition of acid injection. By the end of acid injection, conductivity distribution is calculated by the Deng's correlations presented in section 2.3. The conductivity map from the acid fracture model will be transferred to a reservoir simulation model. At

this time, the conductivity will be treated as a product of the permeability and width of the fracture. Because the reservoir simulation has volume conservation laws on Cartesian grids and has a limitation on the ratio of grid width to grid length, we set w_{limit} equal to 0.1 ft. The permeability in each grid, $k_{fw}(x,z)$ is then calculated by

$$k_{fw}(x,z) = \frac{C_{fD}(x,z)}{w_{limit}}. \quad (10)$$

At the end of the work flow, the prediction of the productivity is given as the result, which helps with evaluating the treatments performance.

3.4 Coupling Fracture Model with Acid Model

There are two coupling steps in the new approach of acid fracture simulation, the coupling between the fracture model and the acid transport and dissolution model; and the coupling between the acid transport and dissolution model and the reservoir simulation model. Those two steps use different parameters to integrate the models.

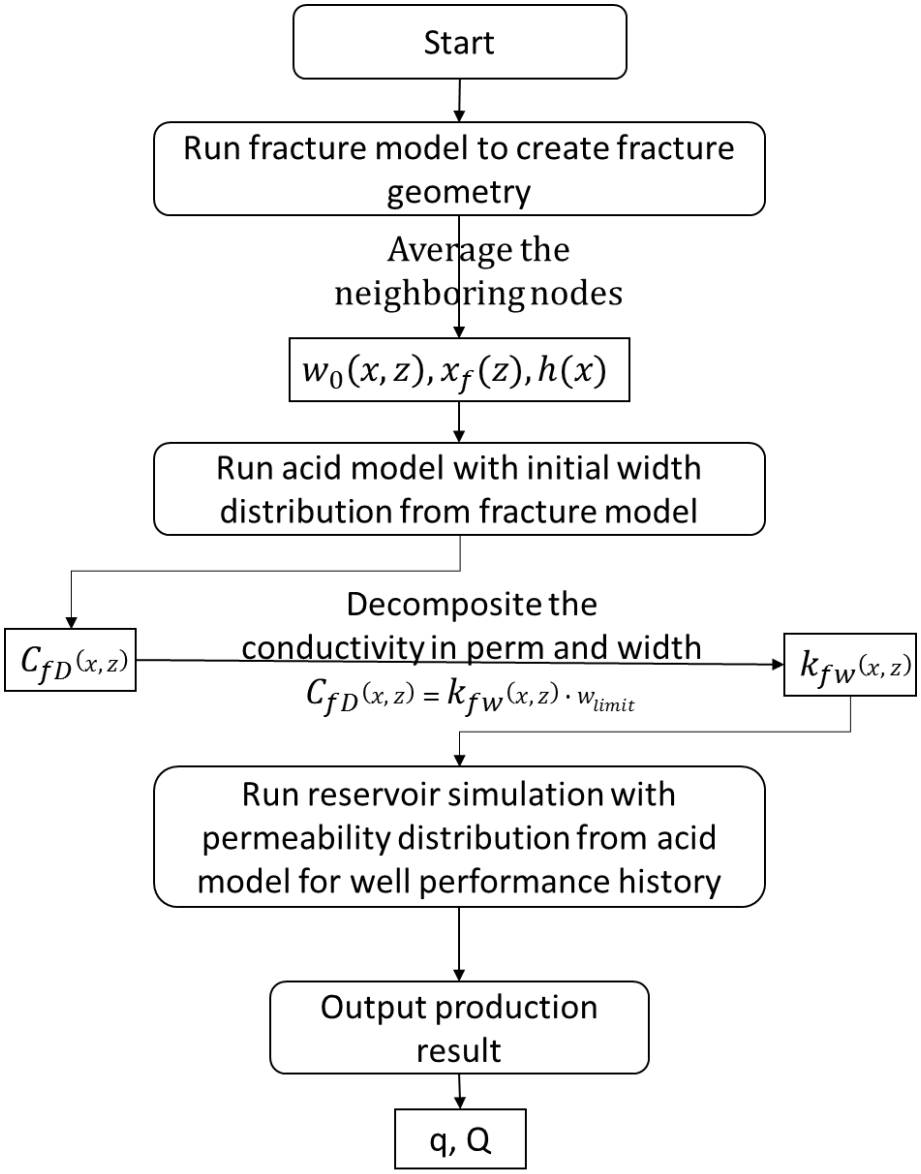

Figure 3.3 Work flow of the new approach

For the link between the fracture and the acid modules, we use geometry data as the coupling parameter. The three dimensions of the fracture define the initial and boundary conditions in the acid model. All fracture models have created fracture geometry data as a part of the output. The coupling data that need to be transferred to the acid model includes $\Delta x\ (i, j)$, $\Delta z\ (i, j)$, and $w\ (i, j)$ on each grid. Here we show how to obtain and process the fracture geometry using the aforementioned commercial software for the acid fracture model.

3.4.1 Fracpro

The fracture geometry can be directly found from the output of Fracpro. Table 3.1 shows an output file example from Fracpro for a fracture geometry at the end of a pad injection. The geometry data is restored in an ".fpx" file, named "PROJECT_NAME.fpx" and can be read using any text editor. For this set of data, the treatment is 158 minutes, and the injection rate is 40 bpm. The width of the created fracture, $w(x, z)$ is presented at locations x (horizontal direction) and z (vertical direction) with constant Δx (15.3 ft.) and Δz (10.1 ft.). Once in the acid model, the local width is further gridded in the y-direction (the fracture width direction) for acid transport and dissolution calculations. Figure 3.4 describes the coordinate system used in this work.

Time=158.2											
Dx=15.3 Dz=10.1											
0.00	0	0	0	0	0	0	0	0	0	0	0
0.29	0.29	0.28	0.27	0.19	0.13	0	0	0	0	0	0
0.41	0.41	0.40	0.39	0.33	0.30	0.27	0.13	0	0	0	0
0.48	0.48	0.48	0.47	0.42	0.40	0.37	0.29	0.22	0.12	0	0
0.55	0.55	0.54	0.54	0.49	0.47	0.44	0.37	0.32	0.26	0.17	0
0.62	0.62	0.61	0.61	0.56	0.54	0.51	0.45	0.40	0.34	0.27	0.15
0.77	0.77	0.77	0.76	0.71	0.68	0.65	0.57	0.52	0.46	0.38	0.26
0.84	0.84	0.83	0.82	0.77	0.74	0.71	0.63	0.57	0.50	0.42	0.30
0.58	0.57	0.57	0.56	0.52	0.50	0.47	0.40	0.35	0.29	0.20	0
0.35	0.35	0.35	0.34	0.29	0.27	0.24	0.14	0	0	0	0
0	0	0	0	0	0	0	0	0	0	0	0

Table 3.1 Example of fracture width output from Fracpro

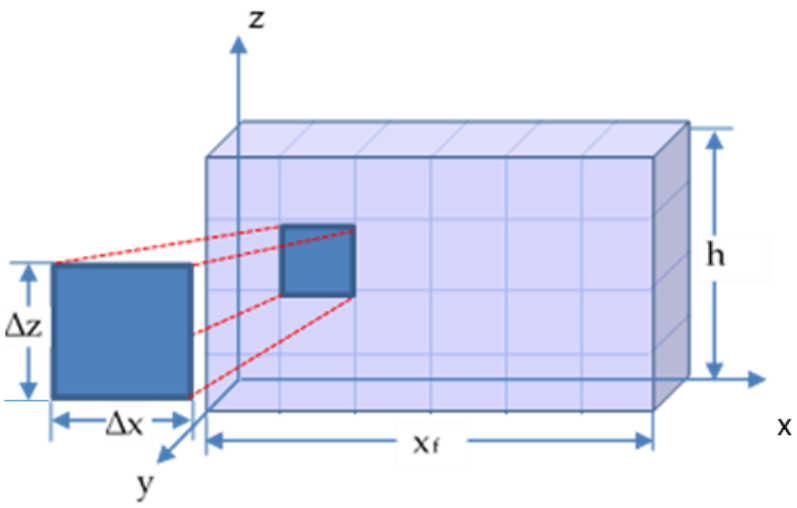

Figure 3.4 Fracture grid coordination system

3.4.2 MFrac

When using MFrac to simulate fracture propagation, an excel file including the fracture geometry data is generated at the end of pad injection. Table 3.2 and Figure 3.5 show an original output of a fracture geometry simulated (both numerical output and dimensional plot).

Notice that the width is presented as a function of x- and z- coordinates, and calculation is needed to change the coordinates to readable grid data before passing it to the acid model. Grid size *dx* and *dz* are calculated by

$$dx = \frac{\sum(x_n - x_{n-1})}{n} \tag{3.2}$$

and

$$dz = \frac{\sum(z_n - z_{n-1})}{n}. \quad (3.3)$$

X(Length-direction)	Z(Height-direction)	Width (in)
0	-113.423	0.066503
8.21291	-113.423	0.065833
16.4258	-113.423	0.065107
24.6387	-113.423	0.064323
32.8517	-113.423	0.063481
41.0646	-113.423	0.062578
49.2775	-113.423	0.061612
57.4904	-113.423	0.060582
65.7033	-113.423	0.059484
73.9162	-113.423	0.058317
82.1291	-113.423	0.057075
90.3421	-113.423	0.055756
98.555	-113.423	0.054354
106.768	-113.423	0.052863
114.981	-113.423	0.051277
123.194	-113.423	0.049587
131.407	-113.423	0.047783

Table 3.2 Fracture geometry numerical output sample in MFrac

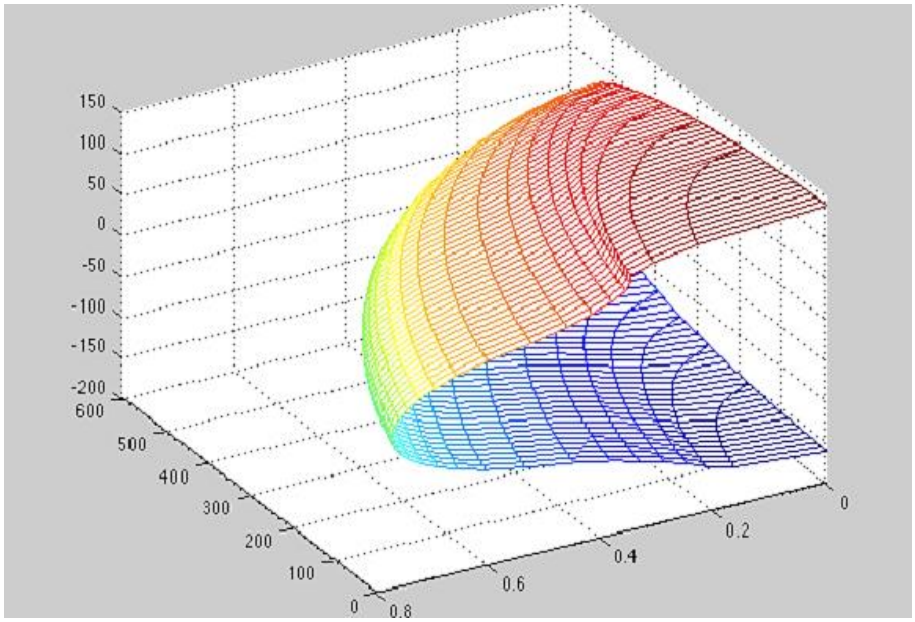

Figure 3.5 Fracture width 3D output from MFrac

3.4.3 GOHFER

GOHFER features flexible grid size (Δx and Δz are not constant), and allows layered stress distributions. Users could adjust the aspect ratio and node size to fit the design. It also has the ability of importing digital log data to configure formation properties, such as permeability, porosity and stress profile, instead of inputting data, as shown in Figure 3.6. This qualifies the small layer variation reflecting in mineralogy composition. The properties of the formation (for example the stress profile, presented in Figure 3.7) could be calculated by the log analysis system.

Adjusting the aspect ratio and grid size, the users can decide the quantity of grids in fracture length and height directions as desired. Applying a designed schedule, a fracture is created. The contour plot of width distribution is shown in Figure 3.8 to illustrate the application. With the width assigned to each block, the geometry model is easily coincided with the acid fracture model without translation. The digital data of the fracture width could be obtained simply by right clicking on the width distribution figure (Figure 3.8) in GOHFER. This information (shown in Table 3.3) can be directly transferred to the acid transport and dissolution model.

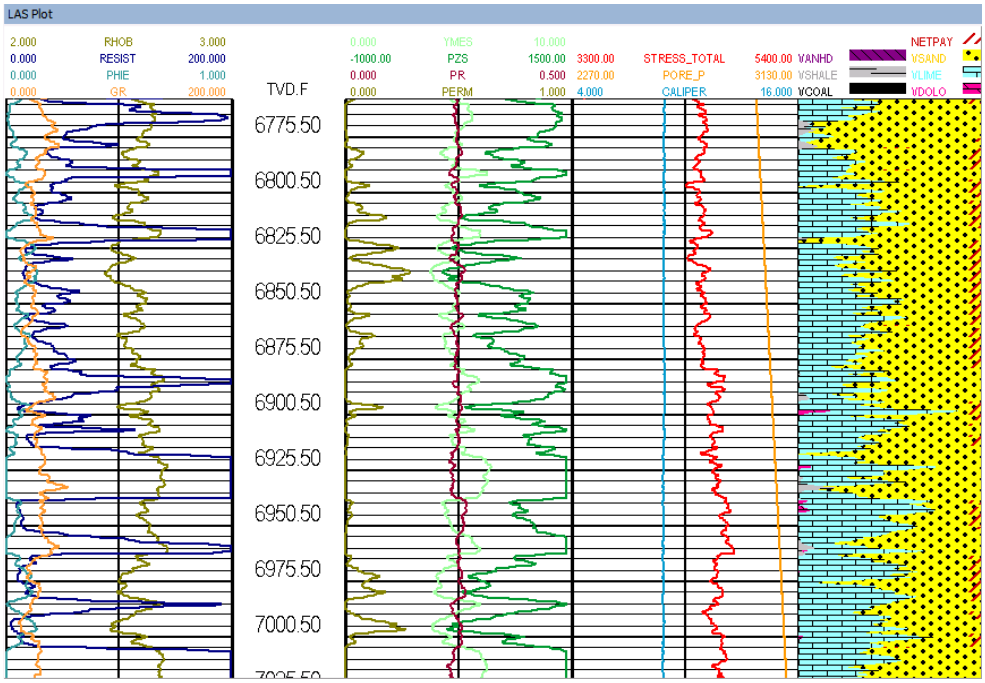

Figure 3.6 Digital log analysis system in GOHFER

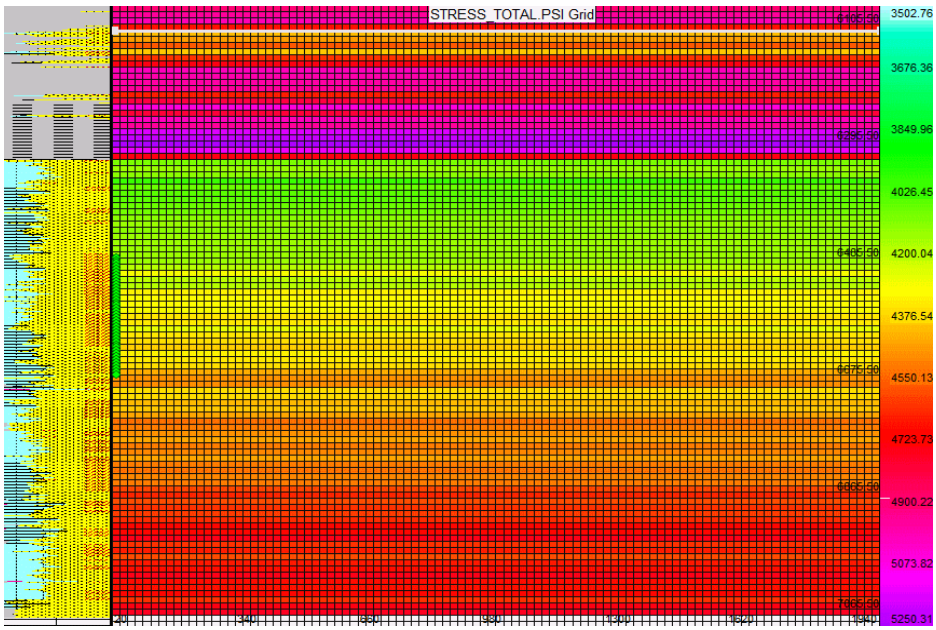

Figure 3.7 Stress profile calculated by GOHFER

0.117	0.116	0.114	0.113	0.112	0.11	0.109	0.107	0.105	0.103	0.101	0.099	0.010								
0.205	0.204	0.202	0.2	0.198	0.196	0.193	0.19	0.186	0.183	0.179	0.176	0.042								
0.234	0.232	0.23	0.228	0.226	0.223	0.22	0.216	0.212	0.207	0.203	0.198	0.193	0.092	0.088	0.084	0.080	0.076	0.071	0.066	0.061
0.241	0.24	0.238	0.236	0.233	0.23	0.226	0.222	0.217	0.212	0.207	0.201	0.194	0.186	0.178	0.17	0.161	0.152	0.142	0.132	0.122
0.221	0.22	0.218	0.216	0.213	0.211	0.208	0.204	0.2	0.196	0.191	0.186	0.18	0.174	0.168	0.161	0.154	0.146	0.138	0.13	0.123
0.22	0.219	0.216	0.214	0.212	0.209	0.206	0.203	0.199	0.195	0.19	0.185	0.18	0.174	0.168	0.161	0.154	0.147	0.139	0.132	0.028
0.225	0.223	0.22	0.217	0.214	0.21	0.207	0.203	0.198	0.194	0.188	0.183	0.177	0.17	0.163	0.156	0.147	0.139	0.129	0.118	0.087
0.225	0.223	0.22	0.216	0.213	0.21	0.206	0.202	0.198	0.193	0.188	0.183	0.177	0.171	0.164	0.157	0.149	0.14	0.13	0.12	0.090
0.227	0.225	0.222	0.218	0.215	0.212	0.208	0.204	0.2	0.195	0.191	0.185	0.179	0.173	0.167	0.159	0.152	0.143	0.134	0.124	0.076
0.186	0.185	0.182	0.18	0.177	0.043															
0.226	0.224	0.221	0.217	0.213	0.209	0.101	0.097	0.093	0.089	0.085	0.081	0.077	0.072	0.067	0.065	0.059	0.001	0	0	0
0.233	0.231	0.228	0.224	0.22	0.216	0.21	0.203	0.196	0.189	0.182	0.175	0.167	0.159	0.15	0.141	0.13	0.076	0		
0.216	0.215	0.212	0.209	0.206	0.201	0.196	0.191	0.185	0.178	0.172	0.166	0.159	0.153	0.145	0.138	0.13	0.053	0		
0.224	0.223	0.221	0.217	0.213	0.209	0.203	0.196	0.189	0.182	0.175	0.168	0.161	0.154	0.146	0.138	0.13	0.12	0.017	0	
0.209	0.208	0.206	0.203	0.199	0.194	0.189	0.183	0.177	0.17	0.164	0.157	0.15	0.143	0.136	0.13	0.124	0.027			
0.040																				
0.045																				
0.201	0.099	0.097	0.094	0.092	0.089	0.086	0.083	0.080	0.077	0.074	0.072	0.016								
0.209	0.207	0.203	0.198	0.192	0.186	0.18	0.174	0.168	0.161	0.155	0.15	0.145	0.010							
0.037																				
0.006																				

Table 3.3 A width profile from GOHFER

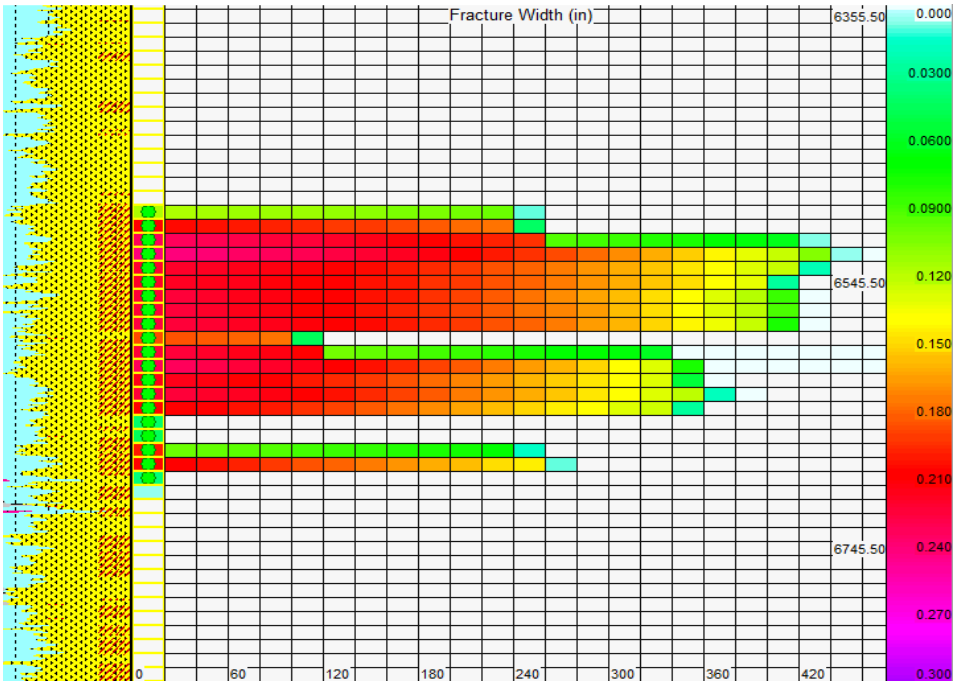

Figure 3.8 Fracture width profile in GOHFER

3.4.4 E-StimPlan

For E-StimPlan, similar output format as Table 3.1 (Fracpro) will be generated and can be imported to the acid model after averaging the width assigned to the adjacent grid nodes to reconcile all the grid systems in models. When selecting the gridding system, Cartesian system is recommended for an easy connection to the acid model. The user may define the grid block sizes before running E-StimPlan. It is suggested that grid block sizes should be greater than 10 feet in each dimension for

coupling with the acid fracture model, which is the one of limitation of the acid fracture model used in this thesis.

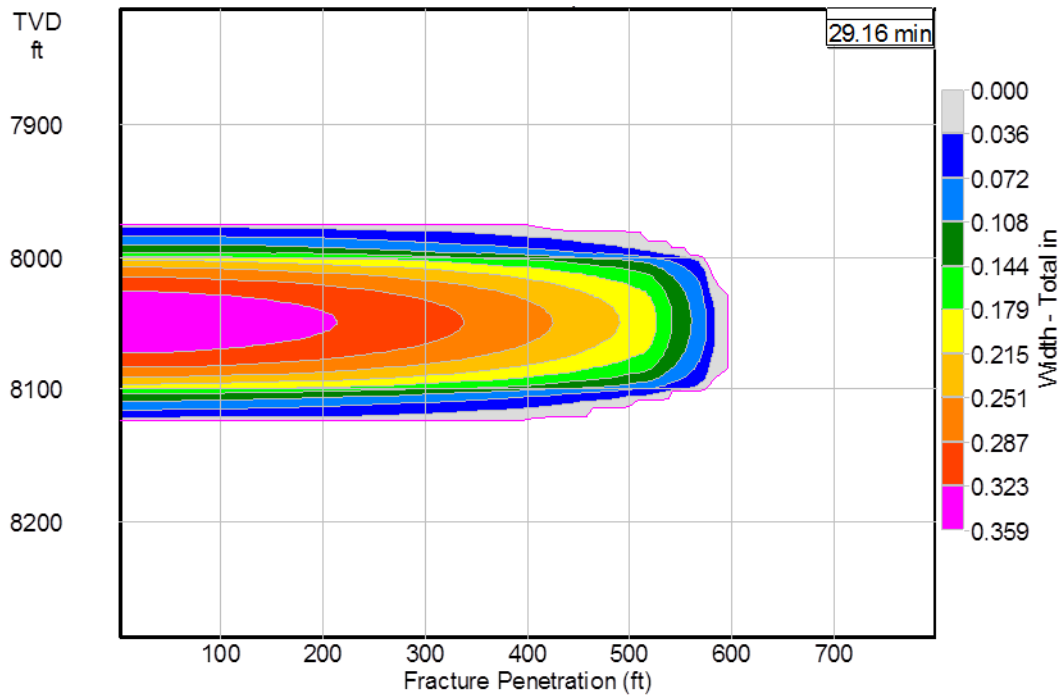

Figure 3.9 A width profile from E-StimPlan

CHAPTER IV

CASE STUDIES AND ANALYSIS

In this chapter, two cases will be discussed. Firstly, a synthetic acid fracture example is provided to explain the approach in detail, then, a field case with an acid fracture treatment in well 27-1A located in the Canyon Reef reservoir in Scurry County, Texas is presented.

4.1 Case 1

A synthetic example is used here to illustrate how to apply the methodology to design and evaluate acid fracture treatments. The formation is assumed 100% limestone. Figure 4.1 shows a pictorial description of our example. The input data for the example is listed in Table 4.1. The table is organized in four main section: the well configuration, the heat transfer parameters, the reservoir parameters and treatment schedule, which is according to the interface in Fracpro (It should be noticed that we can use any of the hydraulic fracturing software described in the previous sections.), and most of the data used in this case is based on default values. The well is defined as a vertical well without decline. The perforation zone is located at 8045 ft. Heat

transfer coefficient is set to a default value, because heat transport is not a dominant factor in this work. The lithology properties are all based on the database in Fracpro.

Interface section	Parameters	Value
wellbore configuration	Casing Length (ft)	8045
	Annulus Length (ft)	6000
	Annulus OD (in)	4.767
	Annulus ID (in)	2.375
	TVD (ft)	8045
	Perforation Zone	8045ft ~ 8055ft
	Number of Perfs	50
	Perforation Diameter (in)	0.33
Heat Transfer	Surface Fluid Temperature (°F)	80
	Reservoir Temperature at Frac Center (°F)	250
	Fracture Heat Transfer Coefficient Multiplier	1.0
Reservoir Parameters	Mineralogy	Limestone
	Reservoir Average Pressure (psi)	3500
	Flowing Bottomhole Pressure (psi)	1800
	Thickness of Payzone (ft)	150
	Reservoir permeability (md)	0.57
	Porosity	10%
	Young's modulus at Payzone (psi)	$1x10^6$
	Fracture Toughness ($psi \cdot in^{1/2}$)	500
	Poisson's Ratio	0.3
Treatment Schedule	Reservoir fluid viscosity (cp)	1.6
	Injection temperature (℉)	100
	Pad injection time (min)	27
	Pump rate (bpm)	40

Table 4.1 Input data for the fracture propagation model of case 1

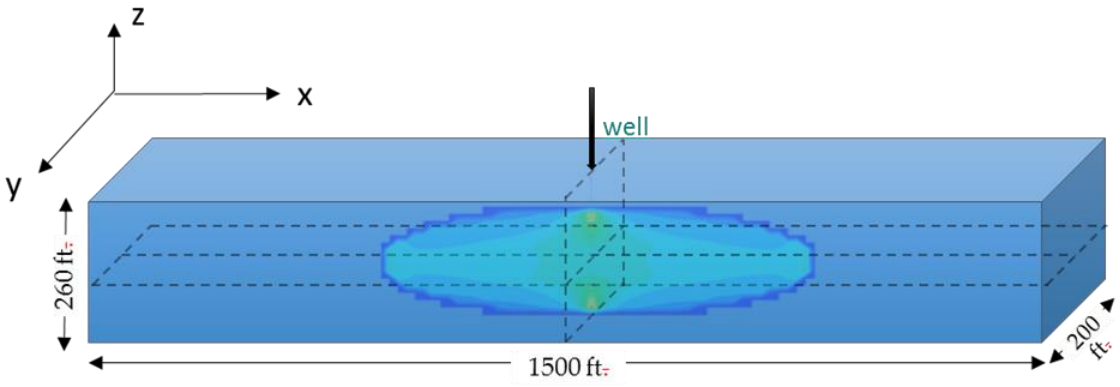

Figure 4.1 Schematic map of case 1

The domain contains a well with one vertical fracture located in a carbonate reservoir bounded by adjacent rocks with higher stiffness. An elliptical shaped fracture was created by the end of hydraulic fracturing. The fracture height is 178.5 ft and the fracture half-length is 350 ft.

Figure 4.2 shows the half-wing fracture geometry and the width at the wellbore. The fracture was assumed symmetric. There are 25 grid blocks in the x-direction (fracture length) and 15 grid blocks in the z-direction (fracture height). The size of each grid is 14 ft in x-direction and 11.9 ft in z-direction. Fracpro can generate the fracture dimension plot as the function of injection time, as shown in Figure 4.3.

Table 4.2 presents the final output that is sent to the acid fracture model. The value in each cell represents the width in inches, where the width is as a function of fracture length x and fracture height z. These values, $w(x, z)$, are arranged in the order of the x-z coordination. Figure 4.4 shows the contour plot of the width distribution.

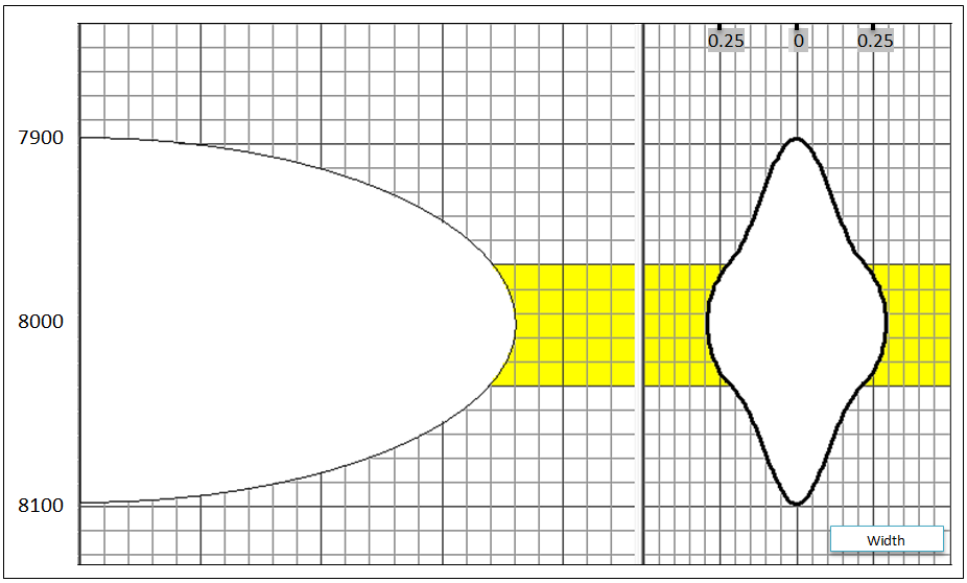

Figure 4.2 Half-wing fracture geometry

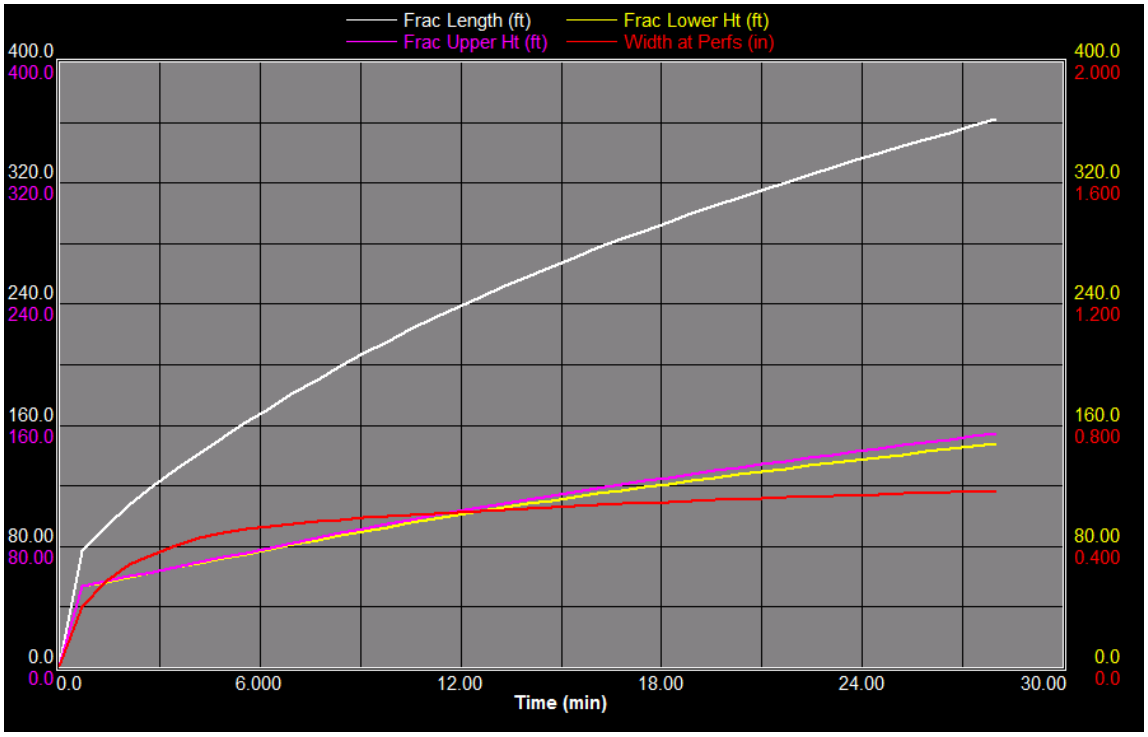

Figure 4.3 Fracture dimension growth as function of time in Fracpro

0.142	0.142	0.140	0.138	0.134	0.130	0.124	0.117	0.108	0.097	0.083	0.065	0.033												
0.208	0.208	0.206	0.205	0.202	0.199	0.194	0.189	0.183	0.176	0.167	0.157	0.146	0.132	0.116	0.095	0.065								
0.266	0.266	0.265	0.263	0.261	0.258	0.254	0.249	0.244	0.237	0.230	0.222	0.212	0.201	0.189	0.174	0.157	0.137	0.112	0.077					
0.330	0.329	0.328	0.327	0.324	0.321	0.317	0.313	0.307	0.301	0.294	0.285	0.276	0.266	0.254	0.241	0.226	0.209	0.189	0.165	0.136	0.096			
0.427	0.427	0.426	0.424	0.421	0.417	0.413	0.408	0.402	0.395	0.386	0.377	0.367	0.356	0.343	0.328	0.312	0.294	0.274	0.250	0.223	0.190	0.147	0.082	
0.530	0.530	0.528	0.526	0.523	0.519	0.514	0.508	0.501	0.493	0.484	0.473	0.462	0.449	0.434	0.418	0.400	0.380	0.358	0.333	0.304	0.270	0.229	0.177	0.096
0.573	0.573	0.572	0.569	0.566	0.562	0.556	0.550	0.543	0.535	0.525	0.514	0.502	0.489	0.474	0.458	0.439	0.419	0.396	0.371	0.342	0.308	0.269	0.220	0.153
0.577	0.576	0.575	0.573	0.569	0.565	0.560	0.554	0.547	0.538	0.529	0.518	0.506	0.493	0.478	0.461	0.443	0.423	0.400	0.374	0.346	0.312	0.273	0.225	0.160
0.542	0.542	0.541	0.538	0.535	0.531	0.526	0.520	0.513	0.505	0.495	0.485	0.473	0.460	0.446	0.430	0.412	0.392	0.369	0.344	0.315	0.282	0.242	0.191	0.117
0.446	0.446	0.444	0.442	0.440	0.436	0.432	0.426	0.420	0.413	0.404	0.395	0.385	0.373	0.360	0.345	0.329	0.311	0.290	0.267	0.239	0.207	0.166	0.108	
0.331	0.331	0.330	0.328	0.326	0.323	0.319	0.315	0.309	0.303	0.296	0.288	0.279	0.269	0.258	0.245	0.230	0.214	0.195	0.173	0.146	0.110	0.051		
0.259	0.258	0.257	0.256	0.253	0.250	0.247	0.242	0.237	0.231	0.224	0.217	0.208	0.198	0.186	0.173	0.157	0.139	0.117	0.087	0.033				
0.197	0.197	0.196	0.194	0.192	0.188	0.184	0.180	0.174	0.168	0.160	0.151	0.141	0.129	0.114	0.096	0.071	0.027							
0.132	0.131	0.130	0.128	0.125	0.121	0.116	0.110	0.102	0.092	0.080	0.064	0.040												

Table 4.2 Fracture width from the fracture geometry model (inches)

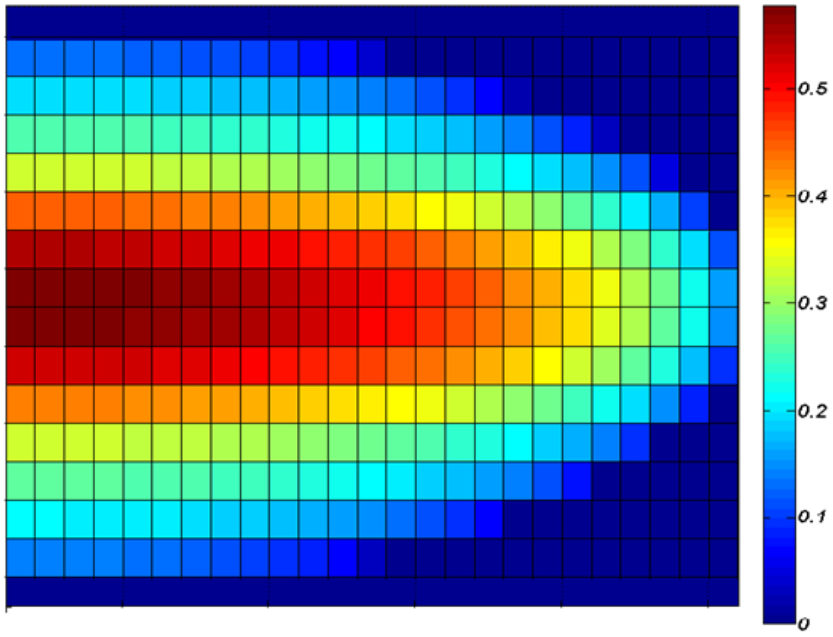

Figure 4.4 Width distribution generated by Fracpro

The next step is to transfer the width profile to the acid fracture model and create acid-etched width profile and conductivity distribution over the fracture domain. The formation is assumed to have a more correlated permeability along the fracture (in x-direction, λ_{Dx}=0.05) and a less correlated permeability in the height direction (λ_{Dz}=0.1). The standard deviation, σ_D, is set to 0.5. Table 4.3 lists the other input data used in the acid simulation.

Figure 4.5 shows the acid-etched width profile after acid injection. The acid etched width is the amount of rock removed from the fracture faces by acid

dissolution. The combined effects of diffusion, convection, and dissolution altered the width distribution from the original width profile generated by hydraulic fracture.

Once the acid-etched width profile is created, we use the conductivity correlations to generate the conductivity profile of the acid fracture. The permeability-dominated correlation Eqs. 1.3 is used in this example, and the acid injection condition is listed in Table 4.3. The final conductivity profile of this example is shown in Figure 4.6.

Parameters	**Value**
Initial Concentration	15 % by weight HCl
Diffusion Coefficient (m^2/s)	$2x10^{-9}$
Injected Fluid Temperature ($^{\circ}F$)	100
Injection Rate (bpm)	40
Injected Time (min)	20
Non-Newtonian Exponent	0.6
Non-Newtonian Flow Index ($kg/m/s^{(2-n)}$)	0.0744
Correlation length in x direction λ_{Dx}	0.05
Correlation length in z direction λ_{Dz}	0.1
Standard deviation σ_D	0.5
Young's Modulus (psi)	$4.5x10^6$
Closure Stress σ_c (psi)	1600

Table 4.3 Acid injection parameters

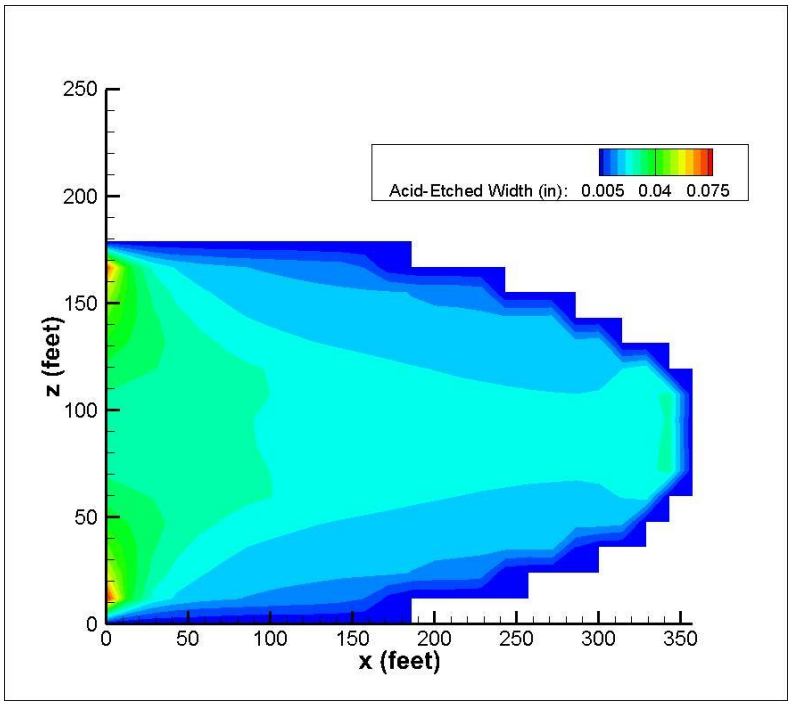

Figure 4.5 Acid-etched width profile

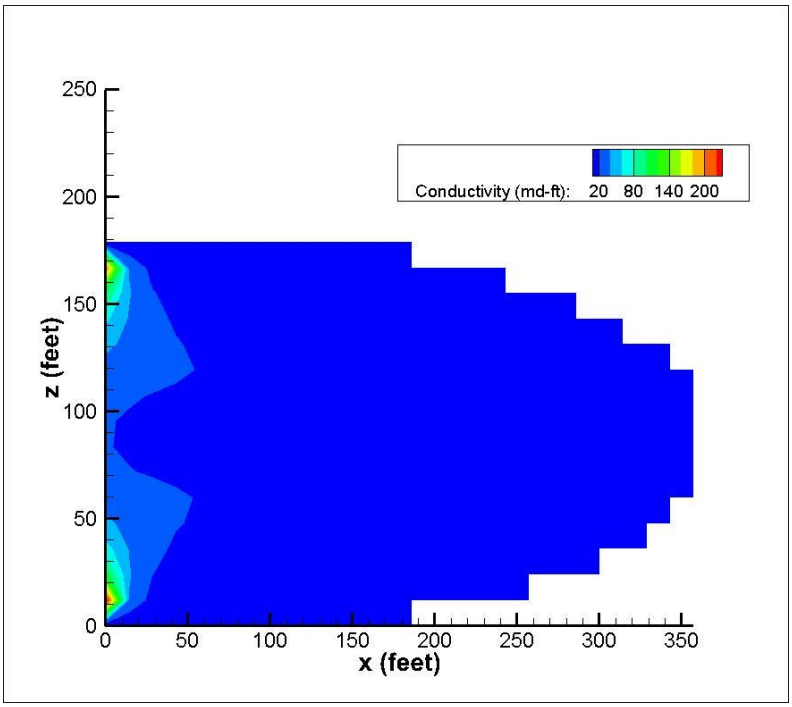

Figure 4.6 Fracture conductivity distribution

The final step is to estimate the productivity for the acid-fractured well by using a reservoir simulator. From the conductivity profile (Figure 4.6) we can calculate the fracture permeability using a fixed width, 0.1 ft, which we have discussed in section 3.1. The permeability profile used in the reservoir simulation is shown in Figure 4.7. Because the fracture width is much smaller than grid size in general, to better represent the fracture, the width of the fracture was enlarged, with the permeability reduced at the same scale to keep the original conductivity value. The fracture used in the reservoir simulation (Figure 4.7) is smaller than the one created after acid etching (Figure 4.5). This is because to distinct fracture to matrix, a cut-off value of permeability is used. The grids with a permeability lower than the cut-off perm are treated as reservoir grids, and the grids with a higher permeability value than the cut-off are treated as fracture grids. The cut-off permeability value of 150 md was used in this example, which trimmed off and in turn, smoothed out, some edge-grids of the acid-etched fracture.

Figure 4.8 and Figure 4.9 show the comparison of production performance of the acid-fractured well for 490 days between the fractured well and non-fractured well. Figure 4.8 is the production rate prediction, and the cumulative production calculated by the simulation is shown in Figure 4.9. It is observed that the treatments enhance the productivity about 80% of the original productivity.

The comparison study between the new approach with the existing fracture simulators which has the acid fracturing model built-in also is illustrated in Figs. 4.8 and 4.9. In this case, Fracpro and E-StimPlan are used to simulate the acid fracturing treatment and predict the productivity with the models built in software packages.

Observing the results shown in Figure 4.9, both the cumulative production calculated by Fracpro and E-StimPlan are less than the one calculated by our model under the same treatment conditions. This difference may be caused by the distinctive acid transport and reaction model employed in three program.

In the acid fracturing models used by commercial software, fluid flow solutions are either two dimensional along the fracture length and height (Barree, 1983; Meyer, 1989; Smith, 2010) or one dimensional (Settari and Cleary, 1984). E-StimPlan provide users to choose whether using the Nierode-Kruk correlation or a University of Texas relation (*E-StimPlan Help Documentation*, 2011). Fracpro solve the acid etching distribution using an integrated velocity to determine the acid concentration throughout a fracture (Settari, 1993). These approaches are based on an influent flow rate with known leakoff subtracted along the fracture length and height. There is no gridding across the fracture width like in our model, so, physical phenomena may be inaccurate modeled. Such gaps might result in different acid etched width calculation

which, in turn, determines the acid fracture conductivity to be included in the simulator model.

Further conductivity decline due to fracture close-up is not considered here. From this point on, the approach can be used to optimize the acid-fracture treatment design based on the production performance response to the treatment.

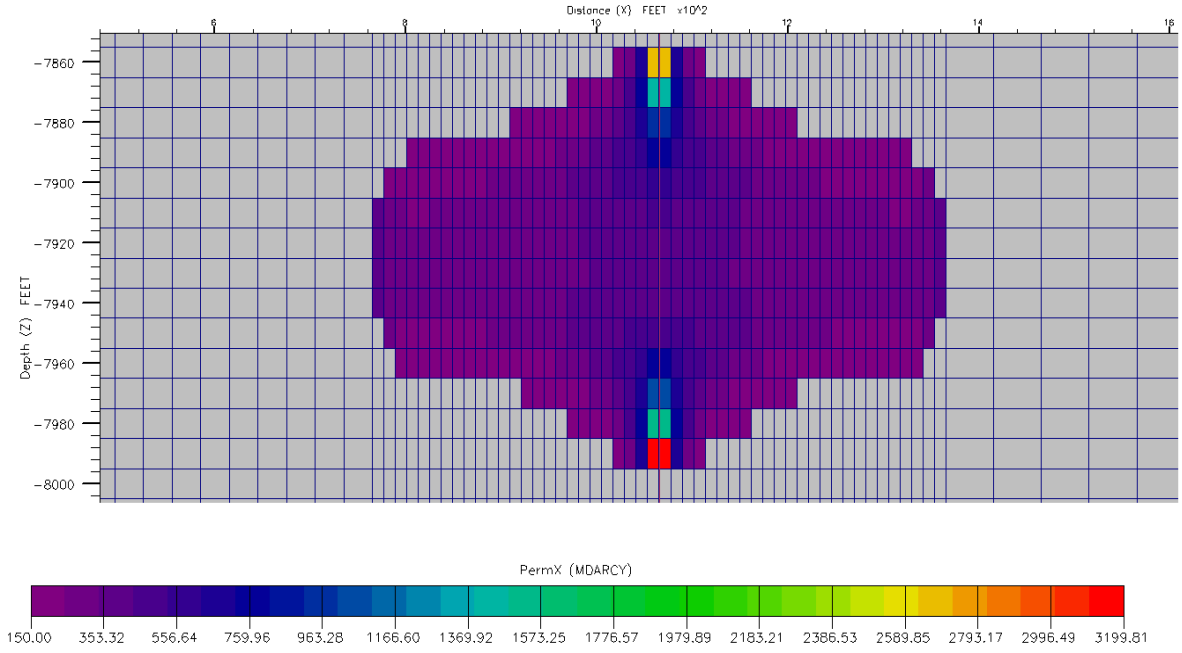

Figure 4.7 Fracture permeability generated for reservoir simulation

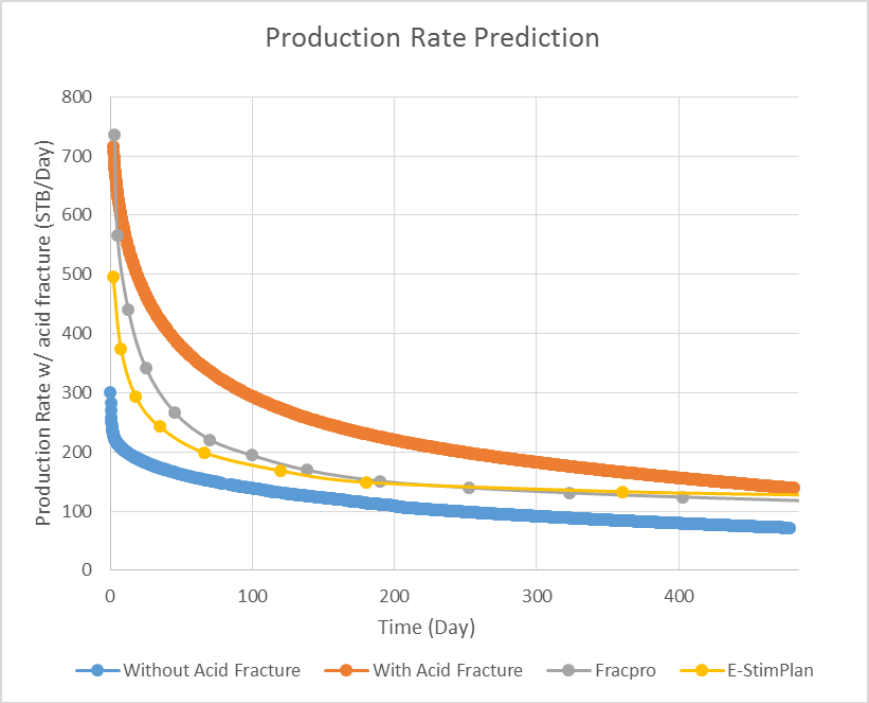

Figure 4.8 Oil production rate for the acid-fractured well and non-fractured well

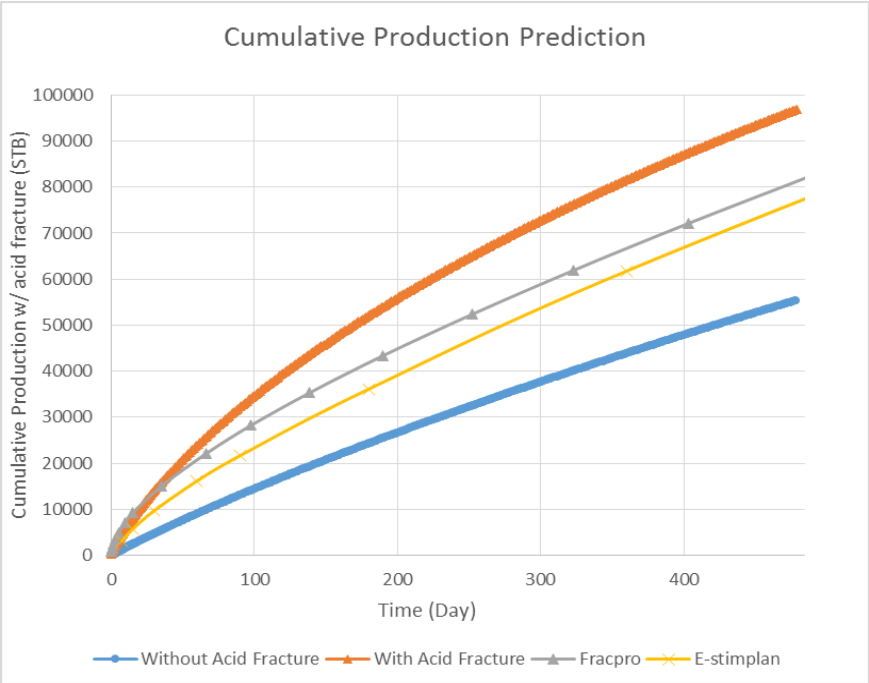

Figure 4.9 Cumulative production versus time

4.2 Case 2: Field Example

This example uses a field case located in the Canyon Reef reservoir in Scurry County, Texas. The formation is a limestone reef with an average producing depth of 6700 feet. Discovered in 1948, the reservoir has since undergone primary, secondary, and is now into tertiary production. Acid fracture treatments are therefore executed for producers and injectors alike.

Well 27-1A is an injector at the crest of the reef structure that communicates with the Middle Canyon layer in the Canyon Reef reservoir. According to the data provided by the service company, the well configuration is drawn in Figure 4.10. The input data of this well is listed in Table 4.4. Most of these values read from the report provided by the company.

The well was firstly stimulated with gelled acid fracture treatments in July 2011. The acid fracturing treatment schedule is presented in Table 4.5.

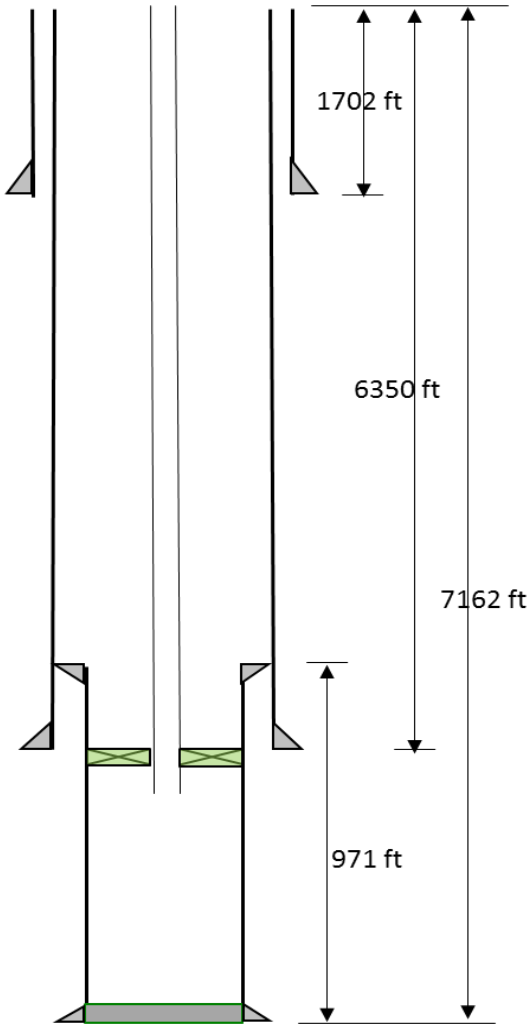

Figure 4.10 Wellbore configuration schematic view

Parameters	Value
TVD (ft)	7162
Perforation Zone	6972ft ~ 7002ft
Number of Perfs	80
Surface Fluid Temperature (°F)	60.9
Reservoir Average Pressure (psi)	2913
Flowing Bottomhole Pressure (psi)	1800
Reservoir permeability (md)	0.571
Porosity	12%
Injection temperature (℉)	128
Average Injection Rate (bpm)	6.5

Table 4.4 Field parameters for case 2

Stage Number	Fluid Description	Volume (bbl.)	Average Pump Rate (bpm)
1	30# crosslinked fluid	4.3	4.4
2	15% by weight gelled HCl	52.1	4.7
3	30# crosslinked fluid	44.3	5.1
4	15% by weight gelled HCl	32.9	7.2
5	30# crosslinked fluid	61.7	5.1
6	15% by weight gelled HCl	10.7	7.7
7	30# crosslinked fluid	23.6	7.9
8	15% by weight gelled HCl	50.2	7.8
9	Flush	106.0	7.8

Table 4.5 Pumping schedule of field case

Using E-StimPlan, the fracture geometry just before the first acid injection stage is presented in Figure 4.11. The fracture width assigned to each node was output to a file which could be read by the acid etching model. Etching is calculated during this displacement to summarize the acid-etched width created during the entire gelled acid stage.

According to the work on this case done by Oeth (Oeth, 2013), the total conductivity is calculated by adding all the etched-width computed after each acid injection stage.

Figure 4.13 illustrates the total acid-etched width map (Oeth, 2013). Figure 4.14 and Table 4.6 show the total conductivity after acid injection treatment.

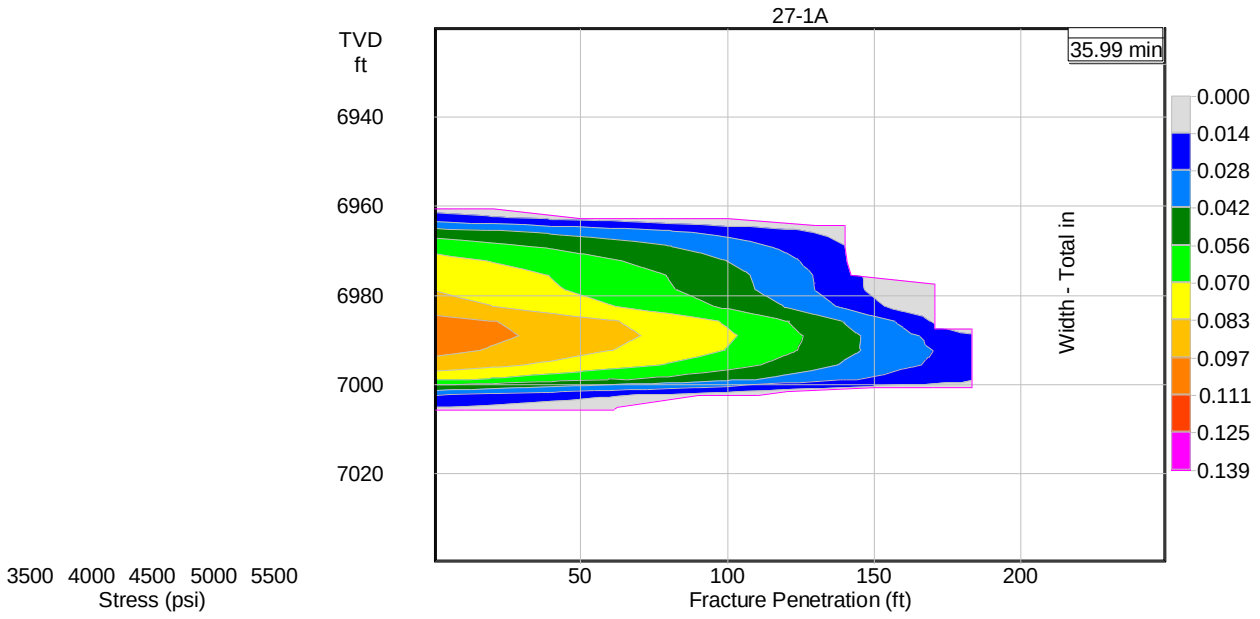

Figure 4.11 Well 27-1A fracture geometry from E-StimPlan

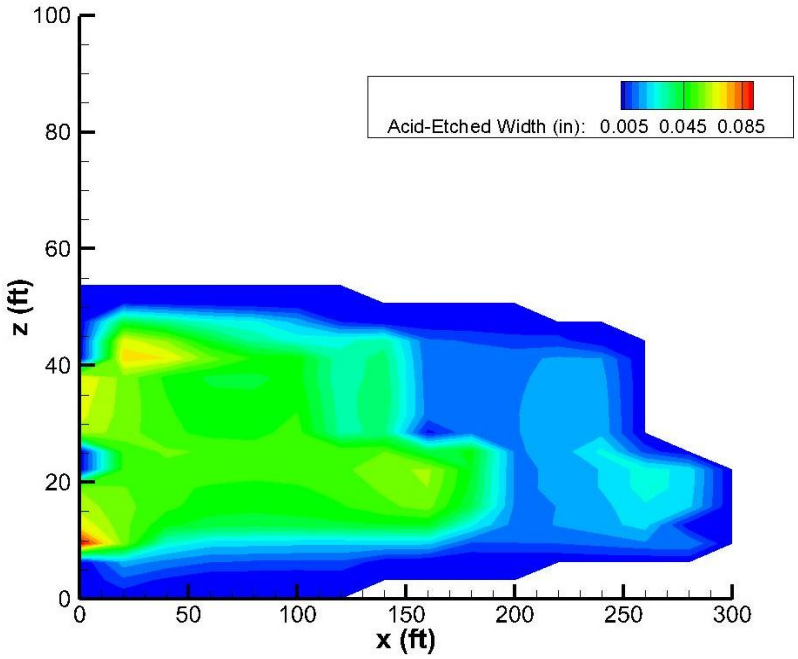

Figure 4.12 Total acid-etched width generated during the multistage acid fracture treatment

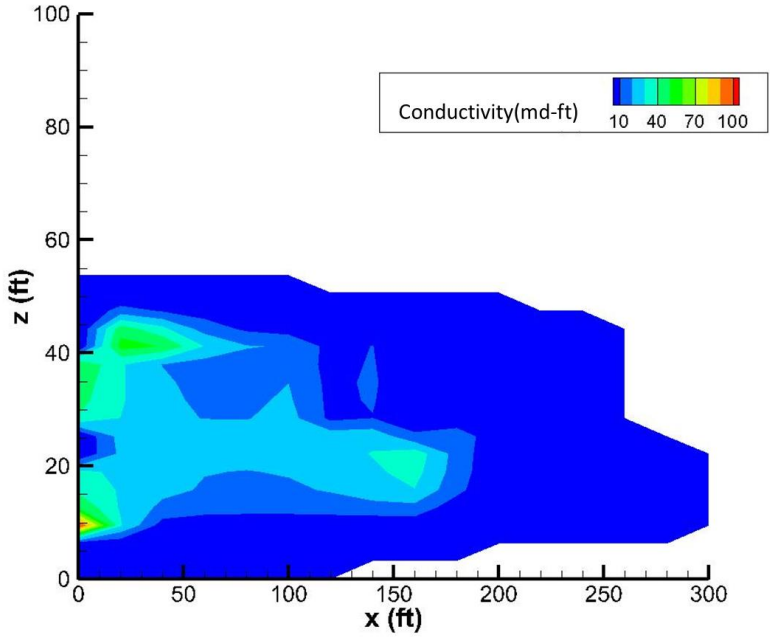

Figure 4.13 Total conductivity generated during the multistage acid fracture treatment

Embedding the permeability separated from the conductivity (as it shown in Table 4.6) into the reservoir simulator, the grid is set up to coincide with the acid model. We assigned the zero-conductivity grids the same permeability as formation permeability. The results of the well performance model are shown as Figure 4.14 and 4.15.

The comparison of the fractured and un-fractured well is presented. The difference is about 80% resulted by the treatments. The trend of production rate (Figure 4.14) declined smoothly after the first month, which is considered reasonable. Further comparative study and history matching is limited for lacking real production history information.

5.7	5.7	31.5	30.0	25.3	5.8	10.6	5.7	5.7
5.7	2.0	47.6	47.6	35.7	28.3	9.0	5.7	5.7
17.7	43.8	22.8	22.8	17.9	16.5	5.8	5.7	5.7
17.5	14.1	11.9	11.9	10.7	11.2	3.9	5.7	5.7
9.8	9.6	9.2	9.3	8.7	7.2	3.7	5.7	5.7
8.2	178.3	163.2	152.7	127.2	42.2	3.2	5.7	5.7
0.2	126.9	356.2	335.6	296.2	168.3	25.2	5.7	5.7
96.3	269.6	305.7	283.6	253.6	162.7	25.3	5.7	5.7
78.6	256.0	258.7	233.0	208.0	153.5	23.9	3.0	5.7
237.4	246.3	242.9	207.0	184.9	144.8	24.3	2.8	5.7
195.3	242.0	237.9	196.7	178.3	135.3	27.6	2.9	5.7
196.3	263.1	249.9	204.0	190.2	142.2	29.0	4.0	5.7
227.5	280.5	252.3	229.3	224.4	176.0	54.0	7.7	0.2
298.8	240.2	222.5	274.7	290.3	289.5	311.7	15.8	2.7

Table 4.6 Equivalent permeability in fracture zone separated from the total conductivity

392.8	5.7	5.7	329.7	377.1	485.6	1027.8	5.7	5.7
298.8	240.2	222.5	274.7	290.3	289.5	311.7	15.8	2.7
227.5	280.5	252.3	229.3	224.4	176.0	54.0	7.7	0.2
196.3	263.1	249.9	204.0	190.2	142.2	29.0	4.0	5.7
195.3	242.0	237.9	196.7	178.3	135.3	27.6	2.9	5.7
237.4	246.3	242.9	207.0	184.9	144.8	24.3	2.8	5.7
78.6	256.0	258.7	233.0	208.0	153.5	23.9	3.0	5.7
96.3	269.6	305.7	283.6	253.6	162.7	25.3	5.7	5.7
0.2	126.9	356.2	335.6	296.2	168.3	25.2	5.7	5.7
8.2	178.3	163.2	152.7	127.2	42.2	3.2	5.7	5.7
9.8	9.6	9.2	9.3	8.7	7.2	3.7	5.7	5.7
17.5	14.1	11.9	11.9	10.7	11.2	3.9	5.7	5.7
17.7	43.8	22.8	22.8	17.9	16.5	5.8	5.7	5.7
5.7	2.0	47.6	47.6	35.7	28.3	9.0	5.7	5.7
5.7	0.0	31.5	30.0	25.3	5.8	10.6	5.7	5.7
5.7	5.7	5.7	5.7	5.7	5.7	5.7	5.7	5.7

Table 4.6 Continued

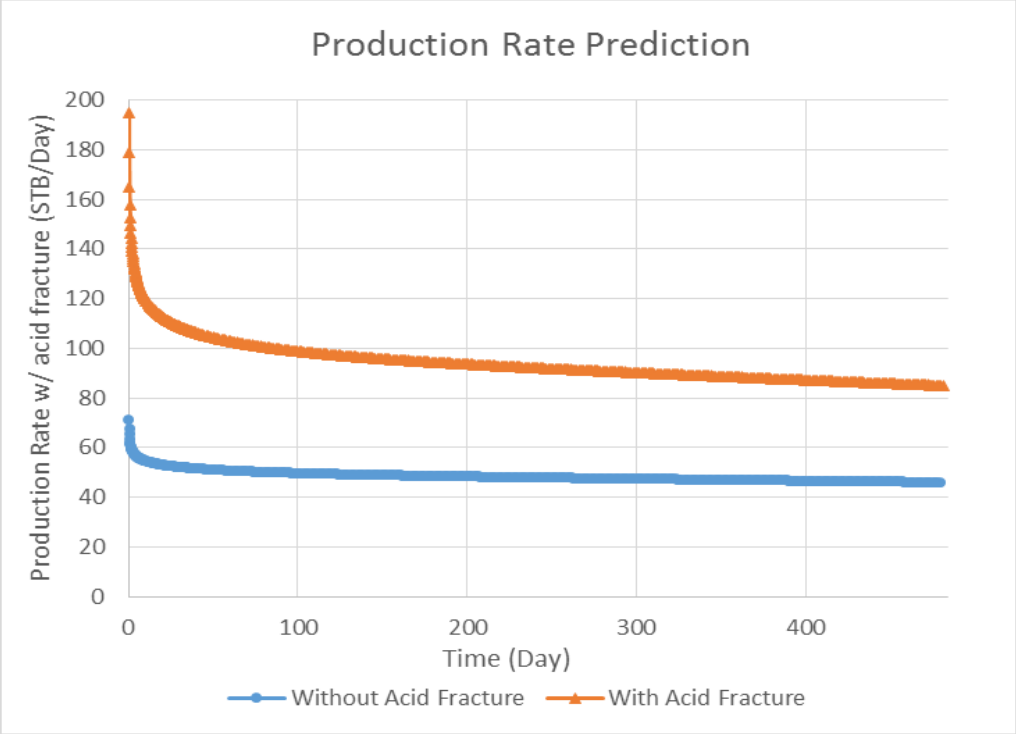

Figure 4.14 Well 27-1A oil production rate

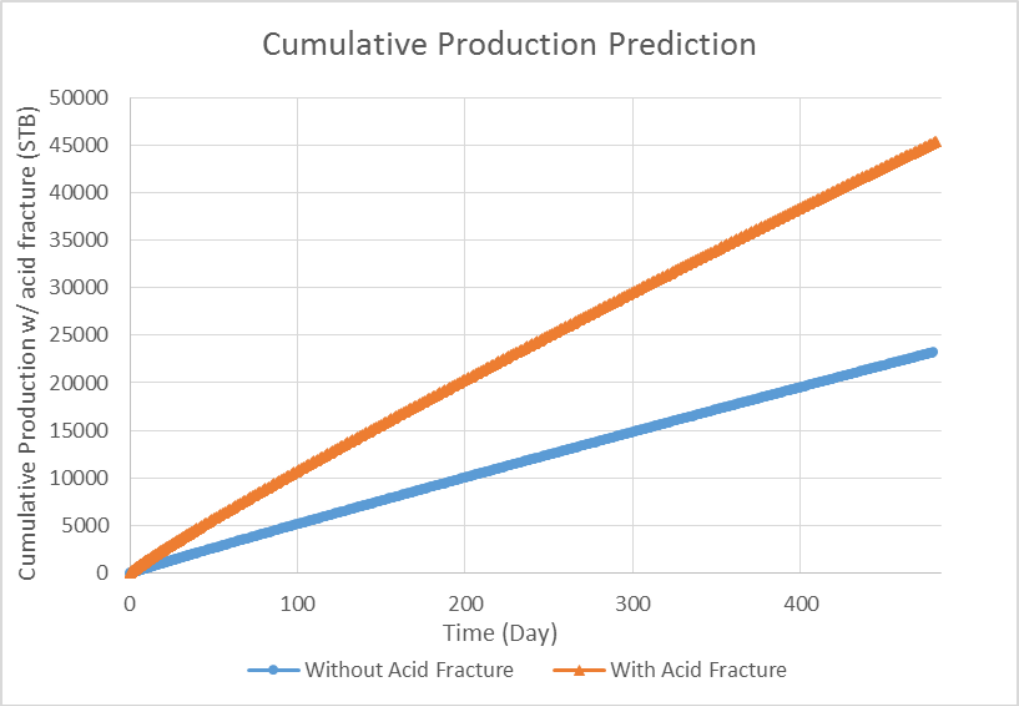

Figure 4.15 Cumulative production

4.3 Summary

In this section, we discussed two cases. The first one is a synthetic case. A vertical acid fracture is designed for a carbonate reservoir. The second is a real case provided by the company. Acid fracturing stimulation is simulated at a limestone reef formation. The workflow is demonstrated by the first case where the full integration is tested in a field case. In both examples, the step-by-step workflow is illustrated thoroughly and in the end comparison was made in terms of production prediction.

The results show that acid fracturing can improve well production rate about 80% for both cases, and even with declined conductivity, treatments are beneficial.

CHAPTER V

CONCLUSIONS AND RECOMMENDATIONS

5.1 Conclusions

The approach presented in this work is a novel paradigm to model acid fracture stimulation. It integrates three individual simulation models in a seamless fashion; a fracture propagation model, an acid transport and dissolution model, and a reservoir simulation model; in order to calculate the performance of acid-fractured wells. A coupling method has been used to create connections between the different models. The effect of geomechanical properties of the rock, and geostatistic properties of a heterogeneous formation are considered in this new approach. The methodology presented in this thesis provides a valuable tool for acid-fracture stimulation design and optimization.

5.2 Recommendations

This thesis proposed a new framework to couple hydraulic fracturing mode with acid fracturing model and reservoir model. However, advanced enhancements could be included in a future continuation of this project.

First, multi-stage fracturing simulation is recommended to be taken into consideration, as in most of real cases, engineers using several injection stages to create a desired fracture profile.

One-way coupling has been achieved in this work. In order to accomplish the original concepts of iterative coupling methods, the feedback of the etched width calculated by the acid transport and reaction model needs to be fed back to the fracture propagation model. In our study, we did not have this capability of changing the fracture propagation model. Thus, two-way couplings need to be thought out for the next steps enhancements of our framework.

Finally, more field cases and comparative study are required to persuade people to trust the reliabilities of the results. In particular, the comparison of the results between the production history and the new approach presented in this work needs to be performed in a more exhaustive way.

REFERENCES

Deng, J., Mou, J., Hill, A.D. and Zhu, D. 2012. A New Correlation of Acid-Fracture Conductivity Subject to Closure Stress. *SPE Production and Operation, 27*(02), P158-169.

Dong, C., Zhu, D. and Hill, A. D. 2001. Acid Penetration in Natural Fracture Networks. Paper SPE 68927 presented at SPE European Formation Damage Conference, The Hague, The Netherlands, 21-22 May 2001.

ECLIPSE (Version 2011.1) [Software]. Schlumberger, Ltd. Houston, TX. Retrieved from http://www.software.slb.com/products/foundation/Pages/eclipse.aspx.

Economides, M. J., Hill, A. D., Ehlig-Economides, C. E. and Zhu, D. 2012. *Petroleum Production Systems*, Prentice Hall PTR, Upper Saddle River, NJ.

Fracpro (Version 2011) [Software]. 2011. StrataGen, Inc. Houston, TX. Retrieved from http://carboceramics.com/fracpro-software/.

GOHFER (Version 8.1.1.0) [Software]. 2010. Barree & Associates, LLC. Lakewood, CO. Retrieved from http://gohfer.com/.

Hagoort, J., Weatherill, B. D. and Settari, A. 1980. Modeling the Propagation of Waterflood-Induced Hydraulic Fractures. *SPE Journal, 20*(04), P293-303.

Ji, L., Settari, A., and Sullivan, R.B. 2007. A Novel Hydraulic Fracturing Model Fully Coupled With Geomechanics and Reservoir Simulator. Paper SPE 110845 presented at the 2007 SPE Annual Technical Conference and Exhibition, Anaheim, California, USA, 11-14 November.

Lo, K.K. and Dean, R.H. 1989. Modeling of Acid Fracturing. *SPE Production Engineering, 4*(02), P194-200.

Melendez, M.G., Pournik, M., Zhu, D. and Hill, A. D. 2007. The Effects of Acid Contact Time and the Resulting Weakening of the Rock Surfaces on Acid Fracture Conductivity. Paper SPE 107772 presented at 7th SPE European Formation Damage Conference, Scheveningen, The Netherlands, 30 May - 1 June.

Mayer, B. 1989. Three-Dimensional Hydraulic Fracturing Simulation on Personal Computers: Theory and Comparison Studies. Paper OTC 5961 presented at the 21st Annual OTC, Houston, Texas, USA, 1-4 May.

Meyer 2012 (Version 5.70.2427) [Software]. Baker Hughes, Inc. Natrona Heights, PA. Retrieved from https://www.mfrac.com/releases/2012/.

Mou, J. 2009. *Modeling Acid Transport and Non-uniform Etching in a Stochastic Domain in Acid Fracturing*. Ph.D. Dissertation, Texas A&M University. College Station, TX.

Mou, J., Zhu, D. and Hill, A.D. 2009. Acid-Etched Channels in Heterogeneous Carbonates—A Newly Discovered Mechanism for Creating Acid Fracture Conductivity. Paper SPE 119619 presented at the 2009 SPE Hydraulic Fracturing Technology Conference, The Woodlands, Texas, USA, 19–21 January

Mou, J., Zhu, D. and Hill, A.D. 2010. A New Acid Fracture Conductivity Model Based on the Spatial Distributions of Formation Properties. Paper SPE 127935 presented at the 2010 SPE International Symposium and Exhibition on Formation Damage Control, Lafayette, Louisiana, USA, 10–12 February.

Oeth, C.V., Hill, A.D. and Zhu, D. 2013. Acid Fracturing: Fully 3D Simulation and Performance Prediction. Paper SPE 163840 presented at the SPE Hydraulic Fracturing Technology Conference, The Woodlands, Texas, USA, 4-6 February.

Pournik, M., Zou, C., Malagon, N., Melendez, M. G., Zhu, D. and Hill, A. D. 2007. Small-Scale Fracture Conductivity Created by Modern Acid-Fracture Fluids. Paper SPE 106272 presented at the 2007 SPE Hydraulic Fracturing Technology Conference, College Station, Texas, USA, 29-31 January.

Ruffet, C., Fery, J.J., Onaisi, A. 1998. Acid Fracturing Treatment: A Surface-Topography Analysis of Acid-Etched Fractures To Determine Residual Conductivity, *SPE Journal*, *3*(02), P155-162.

Samier, P. and De Gennaro, S. 2007. A Practical Iterative Scheme for Coupling Geomechanics with Reservoir simulation. Paper SPE 107077 was accepted for presentation at the SPE Europec 2007, London, England, 11-14 June.

Settari, A. 1980. Simulation of Hydraulic Fracturing Processes. *SPE Journal, 20*(06), P487-500.

Settari, A. and Cleary, M. P. 1986. Development and Testing of a Pseudo-Three-Dimensional Model of Hydraulic Fracture Geometry, *SPE Production Engineering, 1*(06), P449-466.

Settari, A. 1993. Modeling of Acid-Fracturing Treatments. *SPE Production & Facilities, 8*(01), P30-38.

Settari, A., Sullivan, R. B. and Hansen, C. 2001. A New Two-Dimensional Model for Acid-Fracturing Design. *SPE Production & Facilities, 16*(04), P200-209.

Smith, M.B., and Klein, H.A. 1995. Practical Application of Coupling Fully Numerical 2-D Transport Flow Calculations with a Pseudo-3-D Fracture Geometry Simulator. Paper SPE 30505 presented at the 1995 SPE Annual Technical Conference and Exhibition, Dallas, TX, USA, 22–25 October.

StimPlan (Version 6.00) [Software]. 2010. NSI Technologies, Inc. Tulsa, Ok. Retrieved from http://www.nsitech.com/index.php/stimplan-software.html.

APPENDIX A

MANUAL FOR FRACPRO

INTRODUCTION

Fracpro is world widely used fracture software. It is well known for its friendly user interface, extremely fast calculation, and concise but helpful report. Unfortunately, the acid fracture part in Fracpro seems not be strong enough.

Thus, what we are going to do is to couple the commercial fracture simulator like Fracpro with our fully 3D, non-Newtonian numerical acid fracture simulator. This connection might help people to know better how the acid fracture growth and the final conductivity distribution after the completion, which differs from any other simulator in nowadays industry.

MAIN METHOD

Use the function that already exists in the commercial fracture software to generate a geometry data file, and then read it by our acid fracture simulator.

This geometry data file describes a fracture without dissolution and closure (or we can say it is a pure hydraulic fracture before closure). To achieve the goal, we need a 'pause' when all the pad (instead of acid, to eliminate the influence on fracture growth from rock dissolution) injected into the pay zone. Then our acid fracture

simulator will do a 'restart' with the created fracture, and calculate the acid etch and closure.

The output file mainly includes the length, width, and height of each grid block that used to simulate the fracture designed.

TUTORIAL

1. Design

Firstly, we do the fracture. In this tutorial, we pick a simplified 'acid frac example', which is located in the example folder of Fracpro.

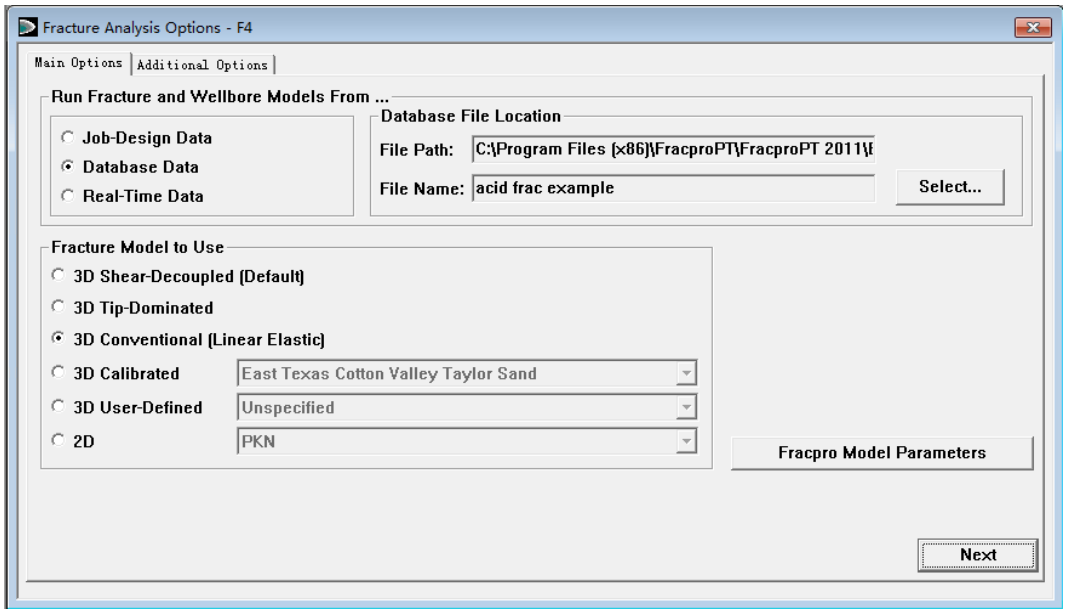

Fill up the well information, the wellbore configuration, the reservoir parameters and Fluid & Proppant selection.

The most different part from the original example is the treatment schedule. As we mentioned above, we need a fracture without rock dissolution and fracture closure. Thus, the schedule should exclude the shut-in period to make sure the simulation will be stopped by the end of acid injection. And select slickwater instead of acid to prevent the simulation calculating the dissolution along the injection procedure.

As the figure shown below, we compared the modified schedule which meets our needs with the original one.

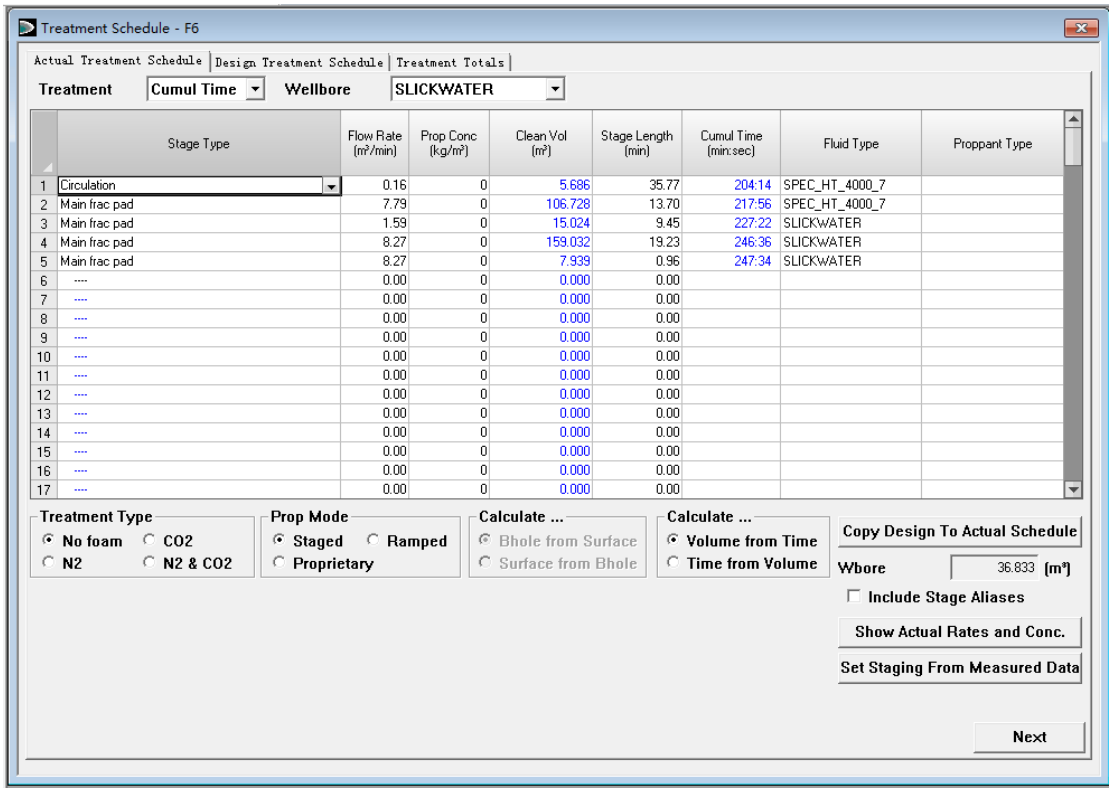

Fig A.1 Modified schedule

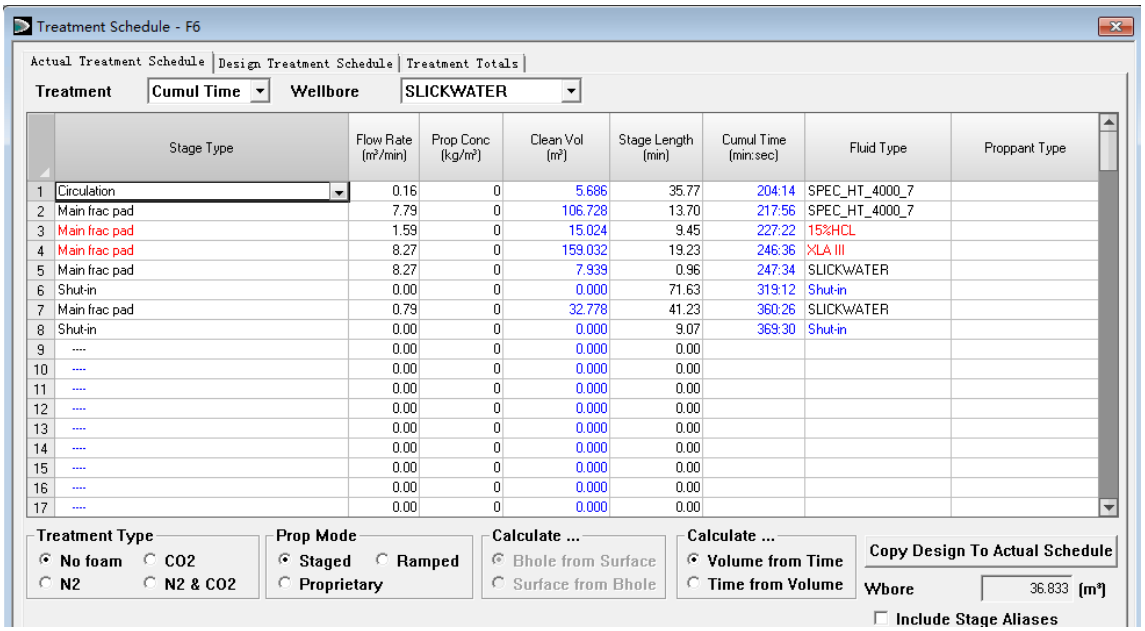

Fig A.2 Original schedule

2. Run Fracpro

Click the 'Run Simulation' bottom to start the simulation.

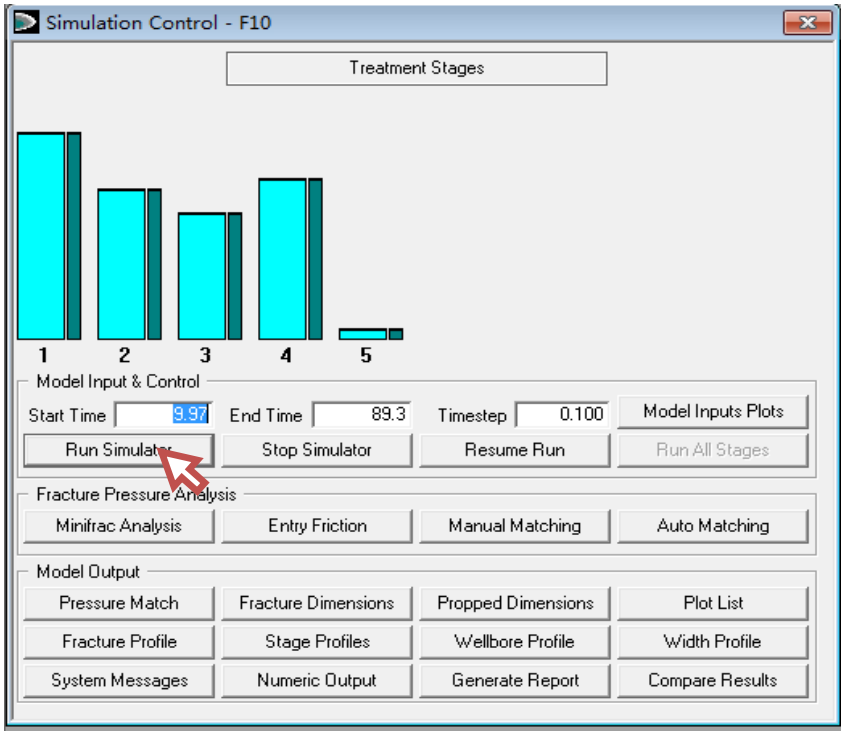

Fig A.3 Control interface

3. Output

Before output the geometry data file, we need to ensure all the windows and interfaces are closed as the figure A.4.

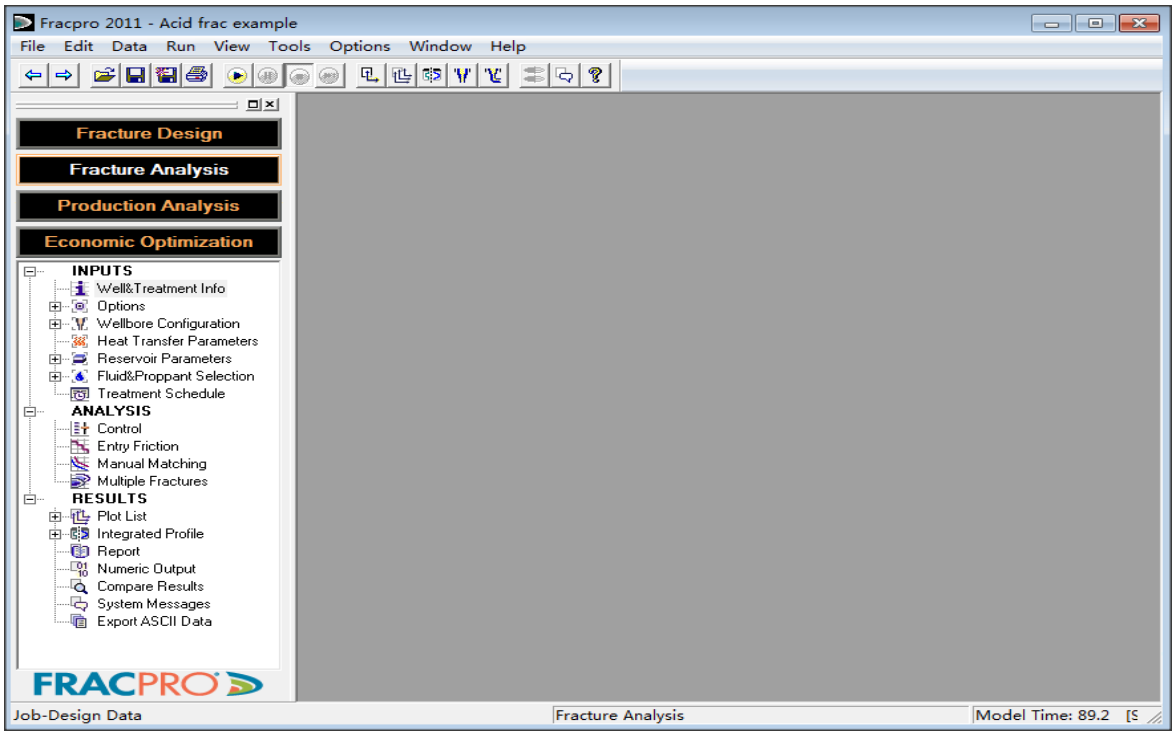

Fig A.4 Preparation for output

Then we select 'Data→Record Model Output'

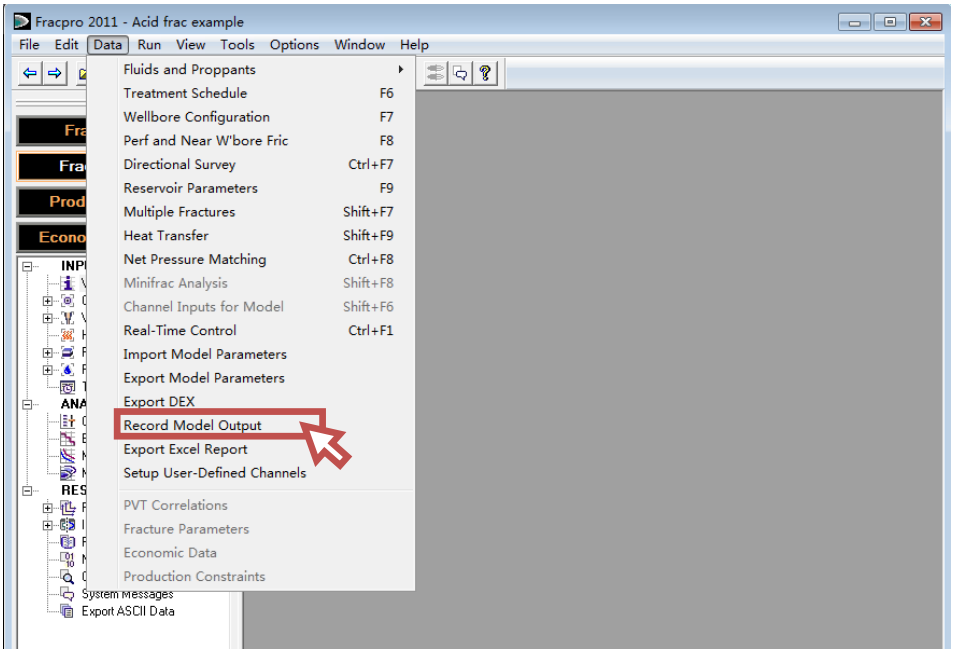

Fig A.5 select the Output function

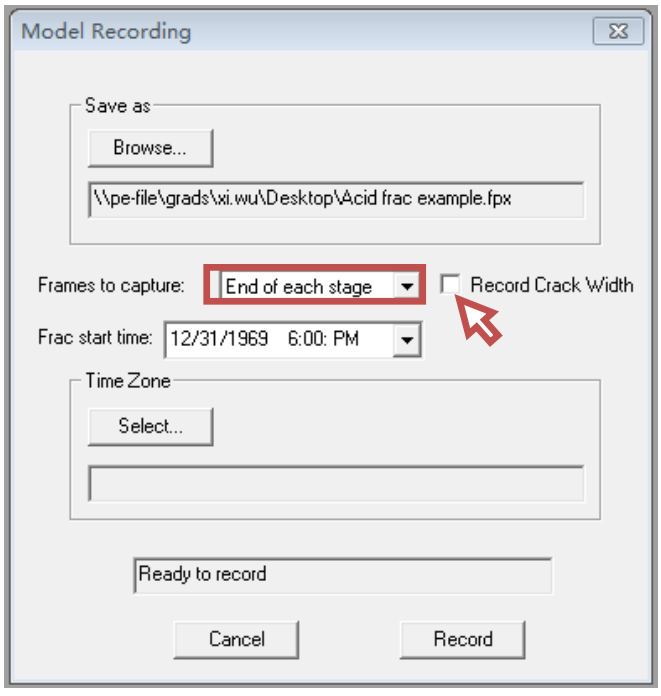

Fig A.6 Check the box before 'Record Crack Width'

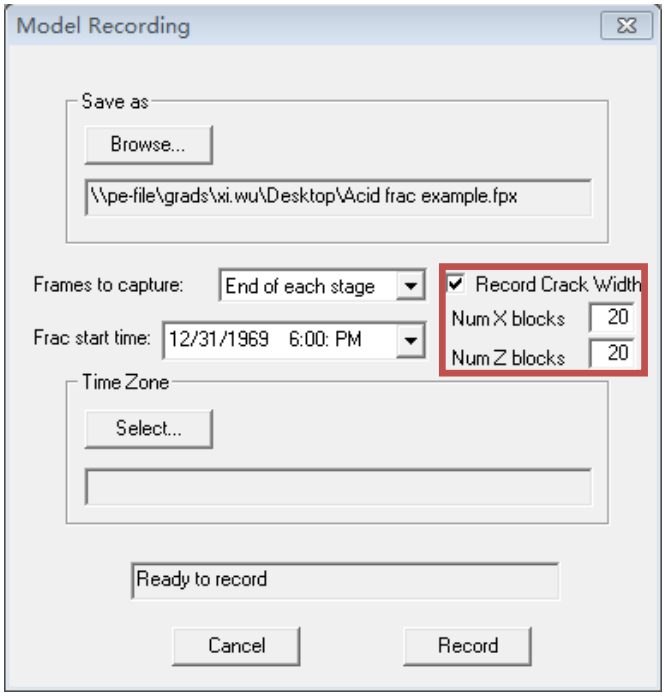

Fig A.7 Set the Grid Block numbers for output

We are able to set the block numbers in X (Length) direction and Z (Height) direction for output by Fracpro. Please choose the appropriate number that fits the area of fracture. The default number is 20.

Click 'Record' to generate the output file. The default folder location is at "C:\Users\[Username]\desktop\"

4. Read

Open the acid fracture simulator to read the output file we have generated in last step. *Due to the grid used by Fracpro is regular Cartesian gridding system. We can read the file directly without any transformation.

APPENDIX B

MANUAL FOR MFRAC

INTRODUCTION

MFrac is the main component of the suite of hydraulic fracture design and analysis software developed by Meyer & Associates. It is popular and high reputation among engineers. Unfortunately, MFrac is not fully 3-D model. Thus, what we are going to do is to couple the commercial fracture simulator like MFrac with our fully 3D, non-Newtonian numerical acid fracture simulator. This connection might help people to know better how the acid fracture growth and the final conductivity distribution after the completion, which differs from any other simulator in nowadays industry.

TUTORIAL

1. Design

Use your fracture design data. As we mentioned above, we need a fracture geometry model to calculate the fracture dimension before acid injection. MFrac runs for non-reactive fluid before acid injection, and the fracture width is then used as the initial condition in acid transport and dissolution modeling. Thus, the schedule should exclude the shut-in period to make sure the simulation will be stopped by the

end of acid injection. And select Pad as stage type instead of acid to prevent the simulation calculating the dissolution along the injection procedure.

As the figure shown below, we change the stage type to 'Pad' of second stage and uniform the acid concentration as 0.

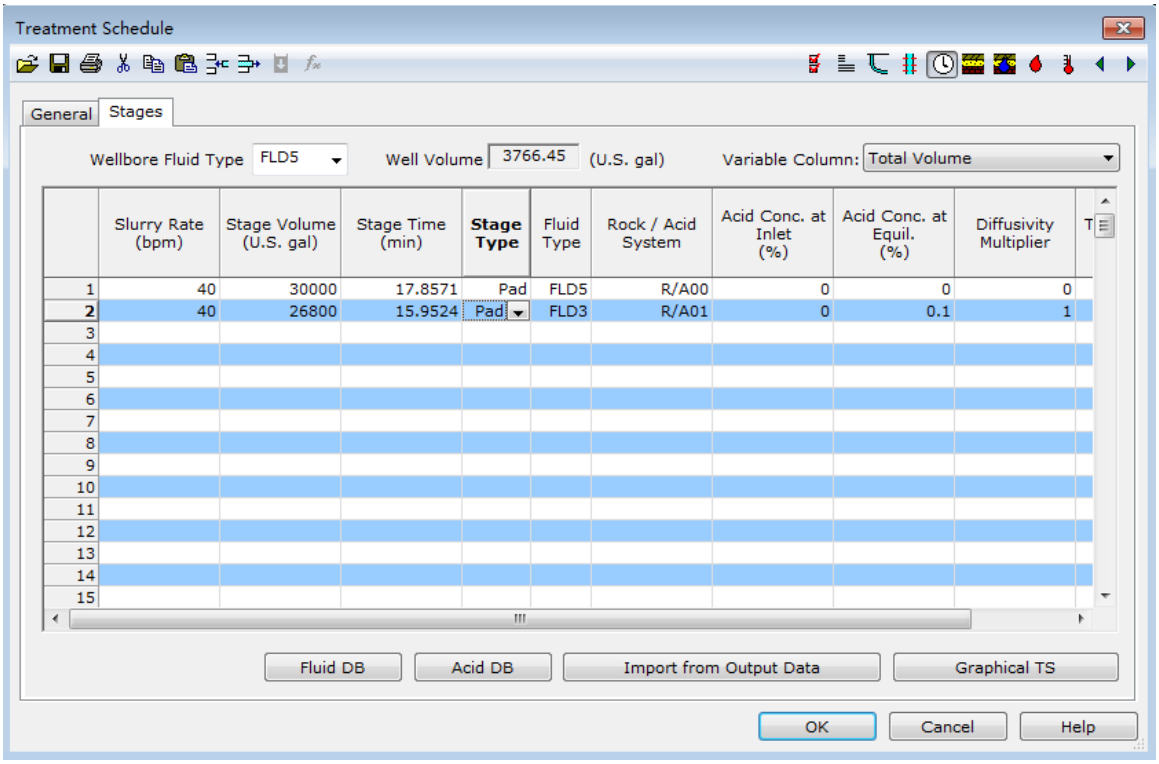

2. Run the simulation

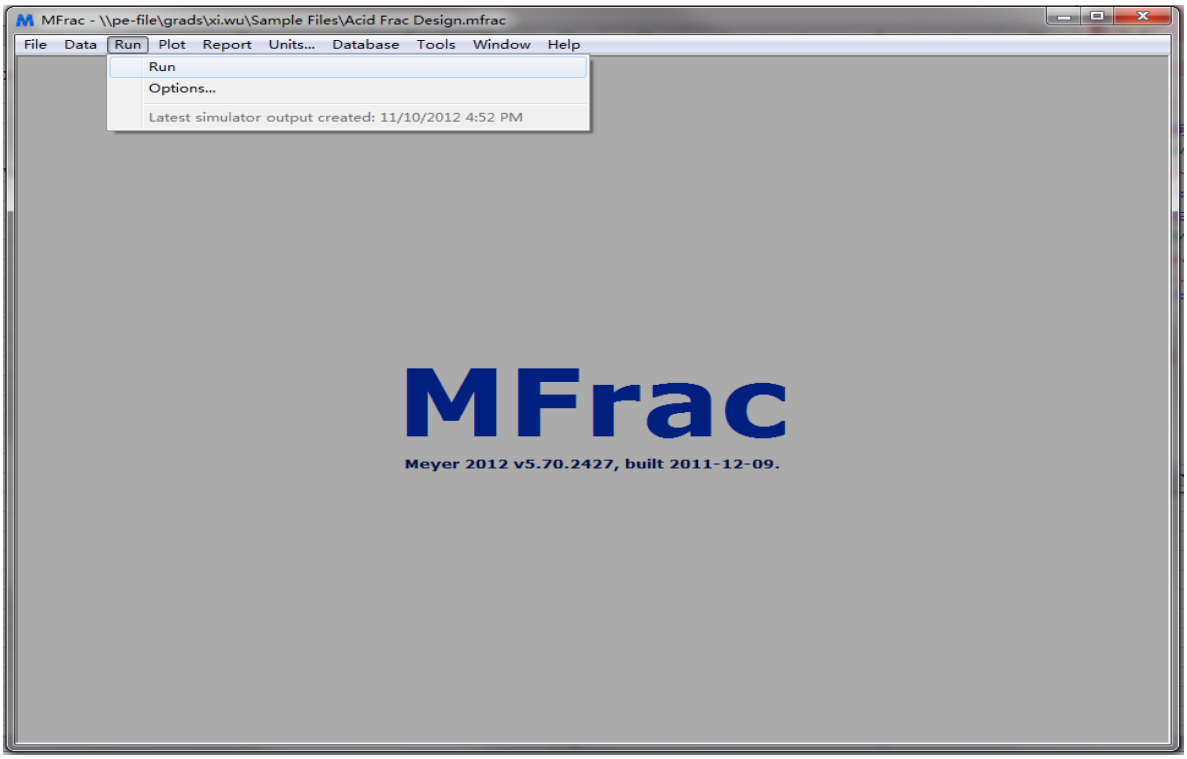

3. Output

To output the geometry data file, we select 'Plot→Three Dimensional'

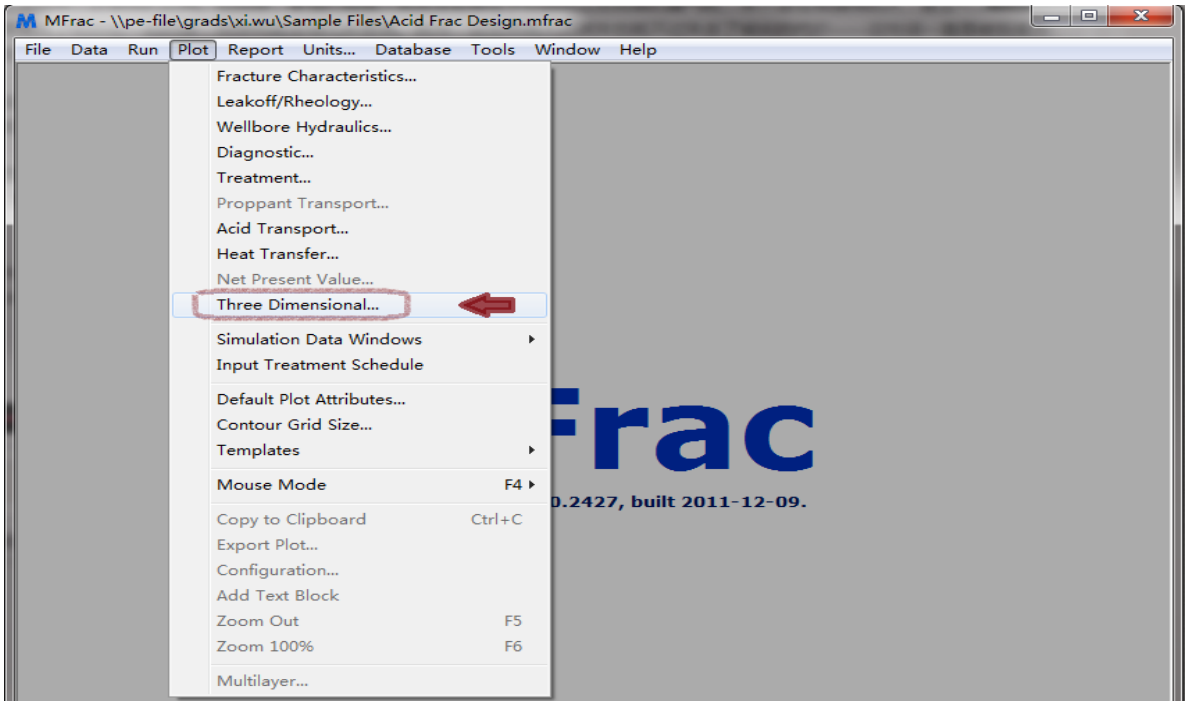

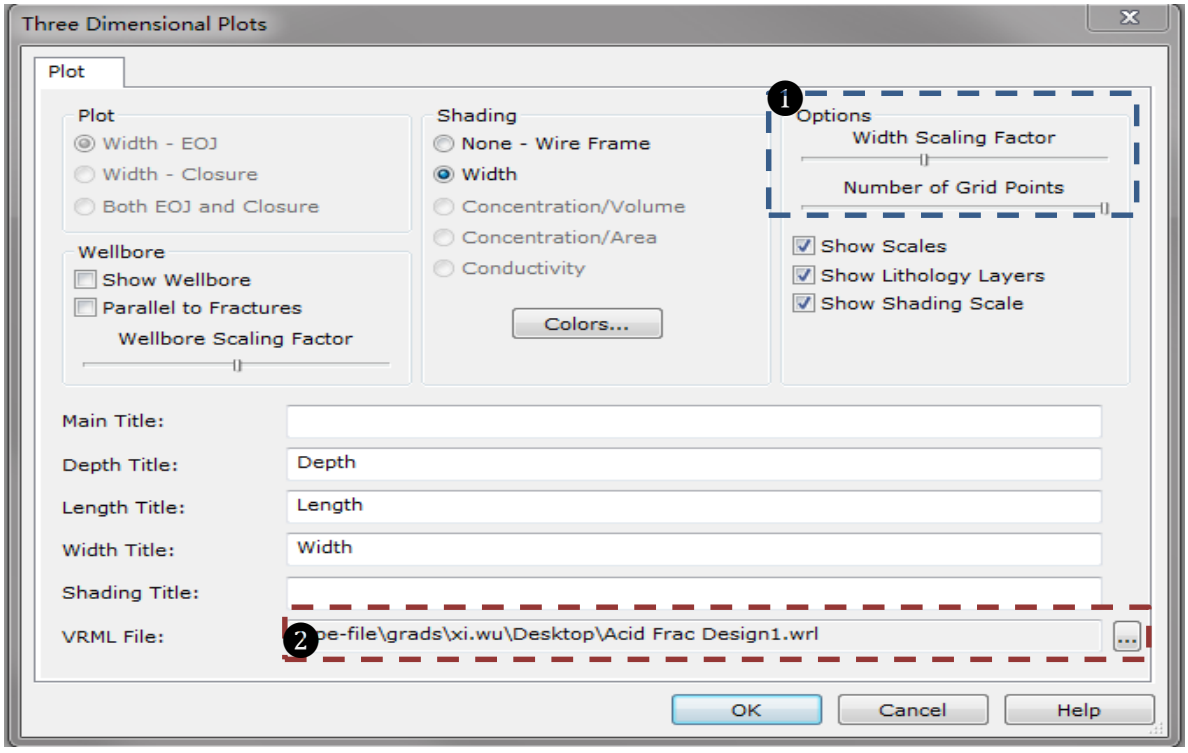

I. For No.1 box, the grid block number option, users may hold and drag the square to adjust the cuboid grid size

II. For No.2 box, the generated file location setting. Click on '…' to change the folder path and file name

III. Click 'OK' to generate the file. Then the Excel will be opened, users might close it.

4. Read

Open the data file located folder, the file ended with ".csv" is what our simulator looking for.

*Due to the grid used by MFrac is regular Cartesian gridding system. We can read the file directly without any transformation.